Urban Forestry & Urban Greening 122 (2026) 129489

Contents lists available at ScienceDirect

Urban Forestry & Urban Greening

journal homepage: www.elsevier.com/locate/ufug

Original article

Remote sensing reveals heterogeneous responses of urban vegetation types to compound heat and drought events in Hamburg, Germany

Nadine Kaul [a,b,*], Nikola Lenzewski [b], Olaf Conrad [a], Jürgen Böhner [a], Kai Jensen [b], Benjamin Poschlod [c,d]

[a] Department of Earth System Sciences, Physical Geography, Earth and Society Research Hub (ESRAH), Universität Hamburg, Bundesstraße 55, Hamburg, 20146, Germany
[b] Department of Biology, Applied Plant Ecology, Universität Hamburg, Ohnhorststraße 18, Hamburg, 22609, Germany
[c] Earth and Society Research Hub (ESRAH), Research Unit Sustainability and Climate Risk, Universität Hamburg, Grindelberg 5, Hamburg, 20144, Germany
[d] Institute for Global Water Security, Hamburg University of Technology, Harburger Schloßstraße 22A, Hamburg, 21079, Germany

ARTICLE INFO

Dataset link: Hamburg Habitat NDVI Deviations During Compounding Hot and Dry Summers (Original data)

Keywords:
Urban greening
Compound events
Drought
Remote sensing
NDVI
Sentinel-2
Climate change
Urban ecology
SPEI

ABSTRACT

During the past decade, Europe has experienced an exceptional number of compounding hot and dry summers, with substantial consequences for agriculture, economy, human health, and natural ecosystems. Especially in highly fragmented urban environments, healthy vegetation plays a key role in mitigating the impacts of heat, yet large-scale studies on the ecological effects of drought often overlook fine-scale patterns needed for local adaptation planning. In this study, we analyze the short-term responses of semi-natural and urban vegetation types in Hamburg, Germany, to the compounding hot and dry summers of 2018, 2020, and 2022 using high-resolution Sentinel-2 NDVI (Normalized Difference Vegetation Index) time series. We find that herbaceous vegetation, such as grasslands, exhibited reductions in greenness during the drought summers, with stronger deviations in locations characterized by drier site conditions. Woody vegetation and wetlands showed no consistent decline, indicating limited short-term responsiveness. Although these patterns align with studies from larger spatial scales, our results reveal considerable variability of responses within vegetation cover types as well as pronounced small-scale spatial heterogeneity of responses. These findings suggest a complex interaction of local site characteristics, plant species composition, and the specific timing of droughts. The observed fine-scale variability of responses emphasizes the importance of high-resolution assessments for identifying locally vulnerable vegetation types and informing targeted adaptation measures in urban landscapes. By integrating two widely used and globally applicable metrics – the NDVI and the Standardized Precipitation Evapotranspiration Index (SPEI) – our approach ensures high transferability across sensor platforms and climatic regions. At the same time, the use of high-resolution Sentinel-2 imagery demonstrates its effectiveness for capturing drought responses in fine-scale urban vegetation patches.

1. Introduction

Climate change has increasingly manifested in the form of more frequent and intense heatwaves and droughts across Europe during the past decades (King et al., 2016; Rousi et al., 2022). After the record-breaking European heat wave in 2003 (García-Herrera et al., 2010), Central and Northern Europe experienced a series of exceptionally hot summers (Christidis et al., 2015; Russo et al., 2015), with 2018 marking an unprecedented heat record in Germany (Zscheischler and Fischer, 2020). These extreme heat and drought events not only impacted human health, from reductions in working capacity with economic implications (García-León et al., 2021) to a rise in heat-related deaths (e.g. Robine et al., 2008; Vicedo-Cabrera et al., 2021), but also affected agriculture (Brás et al., 2021) and natural ecosystems (e.g. Ciais et al., 2005; Bastos et al., 2020; Gampe et al., 2021).

While drought poses a threat to basic physiological processes in plants, it is the combination of reduced precipitation with high temperatures that may particularly damage vegetation. The increased evaporative demand due to higher temperatures compromises vegetation growth (Fu et al., 2022) and increases evapotranspiration, which additionally contributes to soil moisture depletion (Böhnisch et al., 2025). With global warming, evapotranspiration is therefore becoming an increasingly important factor in the formation of droughts (Markonis et al., 2021). Furthermore, earlier vegetation greening due to warmer

* Correspondence to: Ohnhorststraße 18, 22609 Hamburg, Germany.
E-mail address: nadine.kaul@uni-hamburg.de (N. Kaul).

https://doi.org/10.1016/j.ufug.2026.129489
Received 16 November 2025; Received in revised form 4 May 2026; Accepted 5 May 2026
Available online 12 May 2026

spring temperatures increases vegetation water demand earlier in the year and may reduce water resources for the peak season (Wolf et al., 2016).

Events in which multiple hazards, such as high temperatures and meteorological droughts, occur concurrently and in combination exacerbate their individual risk, are referred to as compound events (Zscheischler et al., 2018). When analyzing the frequency or risk of such events, potential dependencies between the hazards must be considered. In much of Europe, including central and northern regions, a strengthening negative correlation between air temperature and precipitation has been observed that substantially increases the probability of co-occurring heat and drought (Zscheischler and Seneviratne, 2017). As a result, climate projections indicate a future increase in the frequency of compounding hot and dry summers that are predominantly driven by high temperatures, where future events in Northern Germany are projected to resemble current compounding hot and dry summers in Eastern Europe (Felsche et al., 2024). Hence, the occurrence probability of compounding hot and dry summers in Northern Germany is projected to drastically increase, leading to more frequent and intense soil moisture droughts (Böhnisch et al., 2025).

Quantifying drought remains a challenge, as droughts are not definable by a single physical parameter, but are characterized by their impacts across various systems and time scales (Wilhite and Glantz, 1985). Whether vegetation is affected by drought depends on a complex interplay between meteorological conditions, hydrological site factors, and species-specific traits (Lawler et al., 2011). Moreover, these interactions vary significantly across temporal and spatial scales, especially in urban spaces where vegetation is highly fragmented, and site conditions and hydrological processes are artificially altered and heterogeneous (Crausbay et al., 2017). It is urban areas, however, where small-scale vegetation patches fulfill many important ecosystem services, such as recreation, thermal regulation, pollution reduction, or ecological functions, many of which can be compromised when, for example, evapotranspiration or leaf area of the vegetation is reduced due to drought stress (Guidolotti et al., 2025; Zhang et al., 2021; Kabisch et al., 2021).

As Germany's second-largest city, Hamburg presents a highly diverse and dynamic mosaic of urban and semi-natural vegetation types, ranging from intensively managed parks and cemeteries to semi-natural grasslands and even forests (Brandt et al., 2025; Lüttgert et al., 2022). The complex urban topography and variation in groundwater depth and soil characteristics result in a high degree of heterogeneity in local hydrological conditions (Schickhoff and Eschenbach, 2018). Moreover, Hamburg's geographic location along the Elbe River and its close proximity to the North Sea exposes the city not only to drought risks but also to various types of flooding. This complex relationship to water poses challenges for urban climate adaptation, as not all feedbacks and relations are fully understood on a detailed spatial scale (Hanf et al., 2025). At the same time, Hamburg's climate is projected to resemble that of Toulouse in South-West France by the end of the century, depending on future climate change (Rohat et al., 2017), which emphasizes the need for adapting the urban green to heat and drought to preserve its important functions.

Plant responses to drought can be investigated using a wide range of approaches, including direct sap flow measurements (Süßel and Brüggemann, 2021; Thomsen et al., 2020), dendrochronological analyses (Vicente-Serrano et al., 2014), ecosystem modeling (e.g. Ciais et al., 2005), and satellite-based measurements. Over the past decades, remote sensing has become a key method for detecting drought conditions and assessing their severity across meteorological, hydrological, and agricultural scales (West et al., 2019). Remote sensing enables the quantification of drought impacts on broad spatial extents (Bastos et al., 2020, 2021; Buras et al., 2020; Vicente-Serrano et al., 2013) and can, combined with e.g. meteorological drought indicators, provide multi-source information that is highly relevant for governmental and administrative decision-making regarding drought mitigation (Dabrowska-Zielinska et al., 2020).

While these large-scale studies have revealed distinct regional patterns in vegetation drought sensitivity and are valuable for broad climate risk projections, they often employ coarse-resolution satellite data, such as MODIS, and therefore lack the spatial resolution to capture vegetation–water-interactions on a detailed spatial scale, neglecting heterogeneous site factors and species composition. However, understanding the responses of fine-scale vegetation types to droughts is crucial to implement targeted adaptation measures for climate adaptation, nature conservation, or to preserve their ecosystem services (Roshani et al., 2022). For this purpose, higher-resolution satellite platforms like Landsat and Sentinel-2 are increasingly used for drought detection and monitoring (Varghese et al., 2021; West et al., 2019). However, these datasets still consist of relatively short time series and pose challenges due to data gaps caused by cloud contamination (Granero-Belinchon et al., 2021), although recent gap-filling and time series reconstruction approaches have proven effective in mitigating these limitations and enabling dense observations (e.g. Zhu and Woodcock, 2014; McMahon et al., 2024). The high spatial and temporal resolution supports a detailed analysis of phenological patterns at local scales, which is promising for urban areas (Shahtahmassebi et al., 2021). Despite this potential, only a limited number of remote sensing studies have investigated drought responses of urban vegetation (e.g. Miller et al., 2022; Leisenheimer et al., 2024; Le Saint et al., 2026), and evidence from Northern European cities is especially limited.

Focusing on the city of Hamburg with its diverse mosaic of vegetation types, we investigate short-term vegetation responses to recent compounding hot and dry summers by using Sentinel-2 NDVI time series, Hamburg's habitat survey data, and the Standardized Precipitation Evapotranspiration Index (SPEI). We aim to analyze (1) how Hamburg's vegetation is affected by heat and drought compound events, and (2) which vegetation types are especially responsive to them in the short term.

2. Data & methods

2.1. Study area & habitat survey data

The city of Hamburg (53.55°N/10.0°E, Fig. 1) is home to more than 1.85 million inhabitants (in 2023) and covers an area of 755 km^2 (in 2022; Statistisches Bundesamt, 2025a,b). Its climate is temperate and humid with a mean annual temperature of 9.6 °C and a mean annual precipitation sum of 771 mm (reference period 1991–2020; Deutscher Wetterdienst, 2023/2024). The soils, formed by glacial and fluvial sediments, are very heterogeneous due to small-scale differences in relief and water conditions in Hamburg and have been strongly modified by anthropogenic influences (Schickhoff and Eschenbach, 2018).

Following this heterogeneity in site conditions, Hamburg features a fine-scale mosaic of diverse vegetation types, which are regularly surveyed and documented by the City's habitat mapping program (Brandt et al., 2025). The data of the habitat survey are publicly available through the Ministry for Environment, Climate, Energy and Agriculture (BUKEA, 2024). Our analyses are based on an updated version provided directly by the authority.

A habitat is defined as a relatively homogeneous and clearly delineable vegetation or structural unit in the field, which can be mapped and digitized using a geographic information system (GIS). For habitats of ecological or conservation relevance, species lists of vascular plants are also recorded. Habitats of similar ecological, structural and floristic characteristics are aggregated using a three-letter code system: the first letter denotes the main habitat category (e.g. W for forest, German "Wald"), the second indicates a subgroup (e.g. WM for beech forest), and the third specifies the precise habitat type (e.g. WMM for beech forest on base-rich soils). Very small habitats that are too small to be mapped individually are often included as secondary types within larger habitats. This study includes only habitats that have been

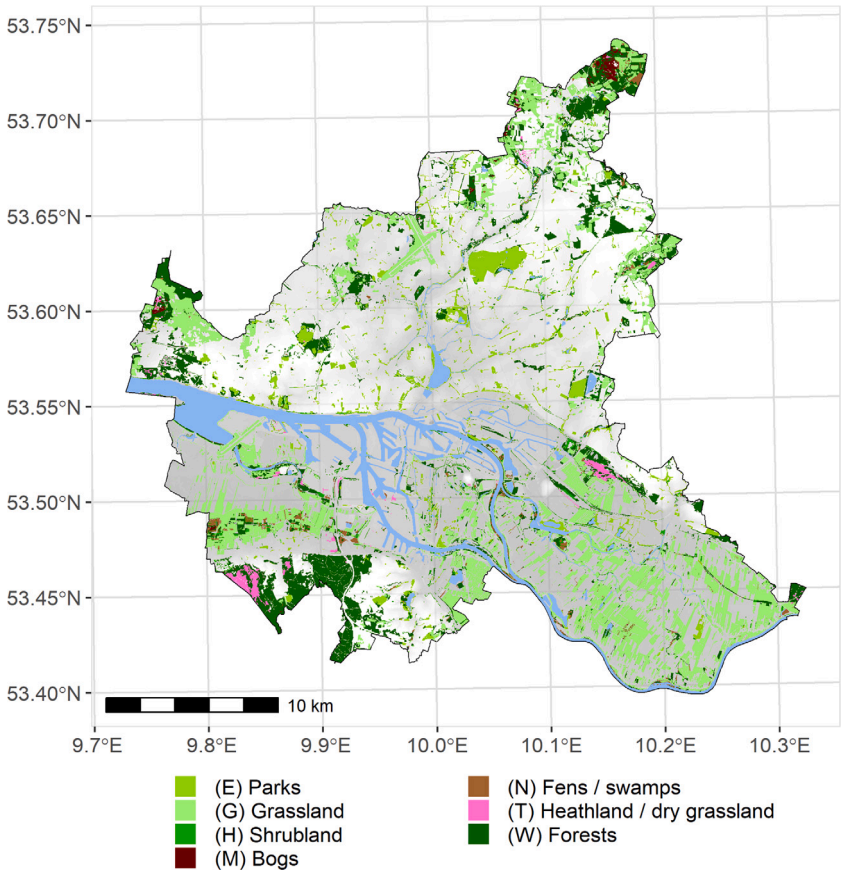

Fig. 1. Spatial distribution of the vegetation cover categories in Hamburg (53.55°N, 10.0°E) included in this study, derived from the city's official habitat mapping survey (Brandt et al., 2025). The included vegetation types encompass semi-natural vegetation as well as urban green spaces such as parks. Water bodies (blue) and elevation (gray shade) highlight the Elbe river floodplains and marshlands. (For interpretation of the references to color in this figure legend, the reader is referred to the web version of this article.)

recorded as areal units, excluding linear and point features such as hedges or singular trees.

Because only a portion of the city is surveyed each year, the dataset is composed of habitat records from different years. For the current analysis, the most recent available entry for each habitat was selected, resulting in a dataset spanning the years 2012 to 2021. To ensure the focus remained on vegetation-driven responses, only habitat types fully composed of vegetation were included, while urban infrastructure (e.g. roads, built-up areas), open water bodies, ruderal patches (typically small and heterogeneous), and agricultural land (often subject to artificial phenological patterns) were excluded. Some non-vegetated or intensively managed types within the main categories were also omitted, such as clear-cut forest areas or playgrounds. The final dataset comprises 13,327 habitats, including semi-natural as well as urban habitats such as vegetated parks and park-like cemeteries. To avoid conceptual ambiguity regarding the biological understanding of "habitats", we instead use the term "vegetation (cover) types" throughout the manuscript.

The spatial distribution of the included main vegetation cover categories is shown in Fig. 1.

To further investigate which vegetation types reacted especially responsive to hot and dry summers, and whether vegetation on wet or dry sites reacted differently, all included vegetation units were additionally assigned to wet, medium, or dry site conditions if the habitat definition in the mapping instructions (Brandt et al., 2025) included information about it. This was the case for most grassland, heathland, shrubland and forest types. Bog, fen and swamp vegetation inherently occurs on wet sites, and could therefore not be further differentiated. For parks, no information about site factors was available in the habitat definitions either. An overview of the spatial distribution of vegetation on wet, medium and dry sites is shown in Supplementary Material, Figure S1.

2.2. Sentinel-2 satellite imagery

To account for the highly heterogeneous and small-scale vegetation structure within Hamburg, our study is based on high-resolution Sentinel-2 data provided by the European Space Agency (ESA). To the time of data acquisition, the Sentinel-2 mission comprised two twin satellites that launched in 2015 and 2017, respectively, and carry multispectral instruments (MSI) that measure the surface reflectance in 13 spectral bands. Among these, the visible and one near-infrared (NIR) bands are available at a spatial resolution of 10 m, making them particularly suited for small-scale vegetation monitoring.

Hamburg is imaged on relative orbit 108 every five days. Due to a swath overlap in higher latitudes, its western part is imaged in between by the adjacent relative orbit 008, enabling a higher revisit time for these areas (see Fig. 2 and Supplementary Material, Figure S2). However, persistent cloud cover remains a major challenge, leaving only about 8% of all Sentinel-2 images completely cloud-free. To address this, we pre-selected images via the Copernicus Browser (Copernicus Data Space Ecosystem, 2025), focusing on images where at least parts of Hamburg's vegetated surfaces were visible. Images with full or dominant coverage of clouds, fog, or snow were excluded; the remaining about 30% of the available Sentinel-2 images from 2015 to 2024 were downloaded as Level-1C Top-of-Atmosphere reflectance products.

Atmospheric correction was performed using the Sen2Cor processor (v2.11) with the recommended default settings (ACRI-ST, 2022), the ESA Climate Change Initiative Land Cover (CCI LC) data package for

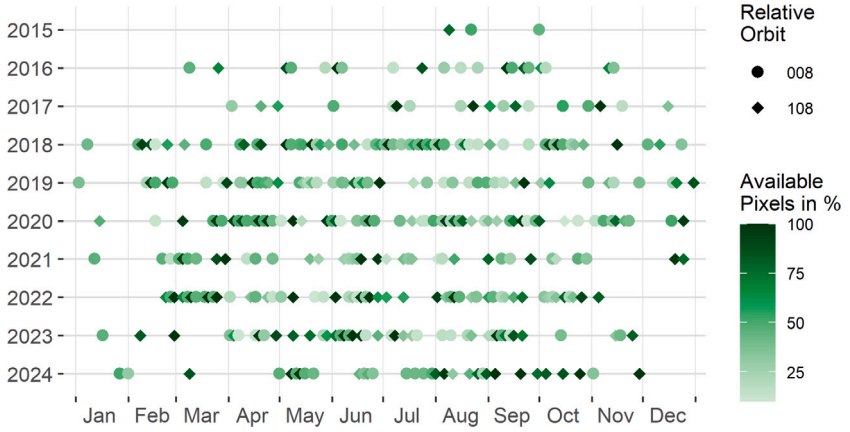

Fig. 2. Sentinel-2 images from 2015 to 2024 included in the study. Images from relative orbit 108 cover the full extent of Hamburg, whereas images from relative orbit 008 include only the western part of the city and therefore cannot exceed roughly 50% of the maximum number of vegetated pixels. The green shading indicates the proportion of vegetated pixels retained after cloud and shadow masking, with darker tones representing clearer scenes and lighter tones indicating increased cloud contamination. (For interpretation of the references to color in this figure legend, the reader is referred to the web version of this article.)

Sen2Cor (Defourny et al., 2017), and the 30 m Copernicus Digital Elevation Model GLO-30 (Copernicus, 2023). Cirrus clouds of each image were removed using the cirrus class of the corresponding Sen2Cor Scene Classification Layer. For cloud and cloud shadow correction, Fmask version 4.6 (Qiu et al., 2019; Zhu and Woodcock, 2012) was used due to frequent misclassification of deciduous forests as shadows by the Sen2Cor Scene Classification in winter images.

To exploit the high resolution of the Sentinel-2 platform, the Normalized Difference Vegetation Index (NDVI; Rouse et al., 1974) was calculated for each pixel in each image using the visible red (RED) and near-infrared (NIR) bands (band 4 and 8, respectively) in 10 m resolution (see Eq. (1)). The NDVI, ranging from –1 (indicating non-vegetated surfaces) to 1 (dense green vegetation), is an established index strongly correlated with leaf area and chlorophyll content (Huete, 2012) and as such widely used in ecological remote sensing and drought monitoring (Le et al., 2023).

$$NDVI = \frac{NIR - RED}{NIR + RED} \quad (1)$$

To exclude non-vegetated pixels from the Sentinel-2 images and to focus the analysis only on the selected vegetation cover types from the habitat survey, a vegetation mask was created. Since the single vegetation units still contain non-vegetated pixels such as roads, bare soil patches, or buildings, we selected two cloud-free images from spring and summer 2023 (19-04-2023 and 08-07-2023, respectively) and clipped them with the selected vegetated areas. We performed K-Means clustering with three and four clusters, respectively, in SAGA GIS (Conrad et al., 2015) on each of the images, using only the visible bands (band 2–4). Clusters were manually classified as either vegetation or non-vegetation. Due to seasonal variability, April images often excluded deciduous forests from vegetation classes, while July images tended to exclude senesced grasslands. Therefore, all pixels that were contained in a vegetation cluster in one of both images were considered to be vegetation and used as a mask to remove non-vegetated pixels from all NDVI images.

After removing clouds, cloud shadows, cirrus clouds and non-vegetated pixels from the NDVI images, all images with less than 10% of potentially vegetated pixels left were deleted, because the leftover pixels can be assumed to still be contaminated by clouds or cloud shadows. The remaining 369 NDVI images contained strongly differing numbers of available pixels (see Fig. 2), which means that the time series for each pixel consisted of a different number of dates (see Supplementary Material, Figure S2).

2.3. Filtering

Despite these masking procedures, individual pixel-based NDVI time series still contained implausible outliers, particularly values close to or below 0, as well as intra-seasonal spikes that likely reflect residual clouds, cloud shadows, or atmospheric noise. To remove these, firstly, all values below 0 were deleted, as they are implausible NDVI values for vegetation. Secondly, all values in a pixel-level NDVI time series were removed if followed by an NDVI increase of more than 0.4 within a 20-day period, as such rapid vegetation greening is ecologically implausible under natural conditions (Chen et al., 2004).

After this outlier filtering, aggregated time series were constructed for each vegetation unit. We therefore calculated medians from all pixels contained in a vegetation polygon per image, if at least half of the pixels were available at that date, and only for units that consisted of at least 10 pixels (7287 units). Dates falling below this availability threshold were considered missing.

Remaining noise and outliers were finally eliminated by a third filtering approach to further smooth the data and improve the reliability of subsequent phenological analyses. For this, we followed the NDVI time series reconstruction methodology proposed by Chen et al. (2004) and adapted to non-uniformly sampled time series like Sentinel-2 by Granero-Belinchon et al. (2020). The methodology uses the Savitzky–Golay-Filter (Savitzky and Golay, 1964) in an iterative procedure that emphasizes high NDVI values and creates a time series that approaches the upper NDVI envelope (Chen et al., 2004). We used the "sgolayfilt" function of the package "gsignal" (Van Boxtel et al., 2021) in R with the parameters proposed as in Granero-Belinchon et al. (2020). Supplementary Material, Figure S3 shows the results of the different filtering steps for all forest-like parks (EPW) as an example.

The iterative filtering approach was originally developed for uniformly sampled time series and thus treats Sentinel-2 time series as if observations were equidistant in time, even though the temporal gaps between cloud-free images vary considerably. As a result, periods with sparse observational coverage tend to be overly smoothed compared to those with higher image availability (Granero-Belinchon et al., 2021). This uneven smoothing effect becomes evident in periods with very few available images, such as 2015 and 2016 when only the Sentinel-2A satellite was in orbit, and is particularly severe in the winter periods of 2015/2016 and 2016/2017, as well as 2023/2024, when cloud cover and snow additionally limited the number of usable images (Supplementary Material, Figure S3 (c)). But it can also be seen in the growing season of 2017, which, despite both Sentinel-2 satellites being operational, yielded very few usable images due to persistent cloud cover (see Fig. 2).

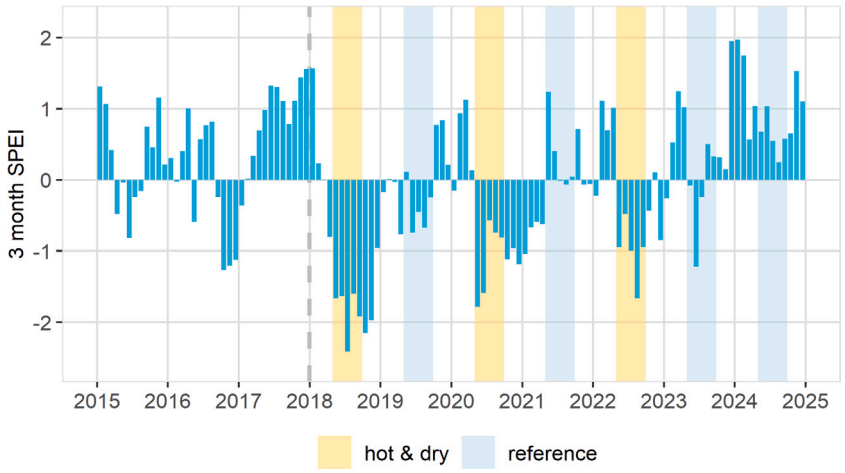

Fig. 3. Three-month SPEI for Hamburg for the years 2015–2024, calculated using the R package "SPEI" (Beguería and Vicente-Serrano, 2023) based on precipitation and evapotranspiration data from the Hamburg-Fuhlsbüttel station of the German Weather Service (DWD Climate Data Center, 2025a,b). The index was computed using a reference period of 1995–2024. Yellow shading indicates summers with compounding hot and dry conditions, blue shading indicates included reference years. (For interpretation of the references to color in this figure legend, the reader is referred to the web version of this article.)

To mitigate these biases and to ensure a more consistent data foundation for phenological and drought impact analyses, we limited the subsequent analysis to the years 2018 onward with more stable data availability and improved spatio-temporal data coverage (see Fig. 2).

2.4. Meteorological data & SPEI

To identify and compare vegetation phenology in drought years with non-drought years, we employed the SPEI (Vicente-Serrano et al., 2010). In contrast to the Standardized Precipitation Index (SPI; McKee et al., 1993), which relies solely on precipitation data, the SPEI is based on the climatic water balance and therefore captures the effect of precipitation deficits and increased atmospheric demand due to higher temperatures, which makes it especially suitable to identify compounding hot and dry summers. In addition, in contrast to other indices that are based on a precipitation–temperature ratio and identify drought in absolute terms (Dabrowska-Zielinska et al., 2021), the SPEI is standardized relative to the local historical distribution of the climatic water balance. It thus identifies summers that are anomalously dry relative to what is normal. Since vegetation is adapted to its baseline climate, drought stress can already be triggered by deviations from that norm, even if the absolute water balance was still positive. Furthermore, the different aggregation periods of the SPEI enable a multiscalar view of drought impacts on meteorological, agricultural, ecological, and hydrological systems (Vicente-Serrano et al., 2012).

Data for monthly precipitation were obtained from records at the weather station Hamburg Fuhlsbüttel (53.6332 N, 9.9881 E) of the German Weather Service (DWD; DWD Climate Data Center, 2025a). Potential evapotranspiration data were provided by DWD based on the Penman–Monteith equation calculated from observations of the same station (Monteith, 1965; DWD Climate Data Center, 2025b). The SPEI was computed for different time scales with the R package "SPEI" with 1995–2024 as 30-year reference period (Beguería and Vicente-Serrano, 2023).

Since the focus of this study was on immediate responses to compounding hot and dry summers, we used the three-month aggregated SPEI to evaluate summer drought conditions (see Fig. 3). We considered years with an average three-month SPEI below −1 in the core vegetation period (May to September) as compounding hot and dry summers. The summer of 2018 emerged as a particularly severe hot and dry one. Additionally, pronounced negative SPEI values occurred in 2020 and 2022. The remaining years were considered non-drought years, but only 2024 showed continuously positive SPEI values and could be considered wet.

2.5. Calculation of reference curve and mean difference

Each hot and dry year (2018, 2020, 2022) was analyzed individually as a phenological NDVI time series. Given the short data record of the Sentinel-2 time series, we established a reference curve for non-drought conditions based on the years 2019, 2021, 2023, and 2024 to facilitate comparability. Therefore, we compiled all NDVI time series from the identified non-drought years and calculated a median value for each day of the year, using linear interpolation between actual observation dates. This produced a continuous phenological reference curve. The phenological impact of each drought year was then quantified by calculating the mean difference between each drought-year curve and the reference curve for each vegetation unit, restricted to the core vegetation period from May 1st to September 30th. Fig. 4 gives an example of the reference and drought curves for species-rich grasslands on fresh to moderately dry sites (GM). For comparative reasons, we additionally calculated the mean NDVI differences based on the period June 1st to September 30th (doy 152–273), excluding May. As a result, three mean difference values were obtained per vegetation unit, one for each drought year. Positive deviations indicate a relative greening compared to the reference curve, while negative deviations represent a reduction in the expected vegetation greenness.

2.6. Statistical evaluation

To identify which vegetation types exhibited responses to compounding hot and dry summers, NDVI mean differences were visualized using boxplots that illustrate the distribution of deviations for vegetation cover types across different aggregation levels. To further assess whether mean NDVI values in drought years differed significantly from the reference curve, we applied the non-parametric Wilcoxon signed-rank test for paired samples (Wilcoxon, 1945) using the function "wilcox.test" from the R package "stats" (R Core Team, 2025). Effect sizes were calculated using the function "wilcoxonPairedR" from the "rcompanion" package (Mangiafico, 2026). The exact results are reported in Supplementary Material, Table S1.

A roadmap outlining all data processing steps is presented in Fig. 5.

3. Results

3.1. Contrasting responses of herbaceous and woody vegetation to hot and dry summers

The NDVI-based analysis of phenological responses to hot and dry summers reveals clear differences between the main vegetation cover

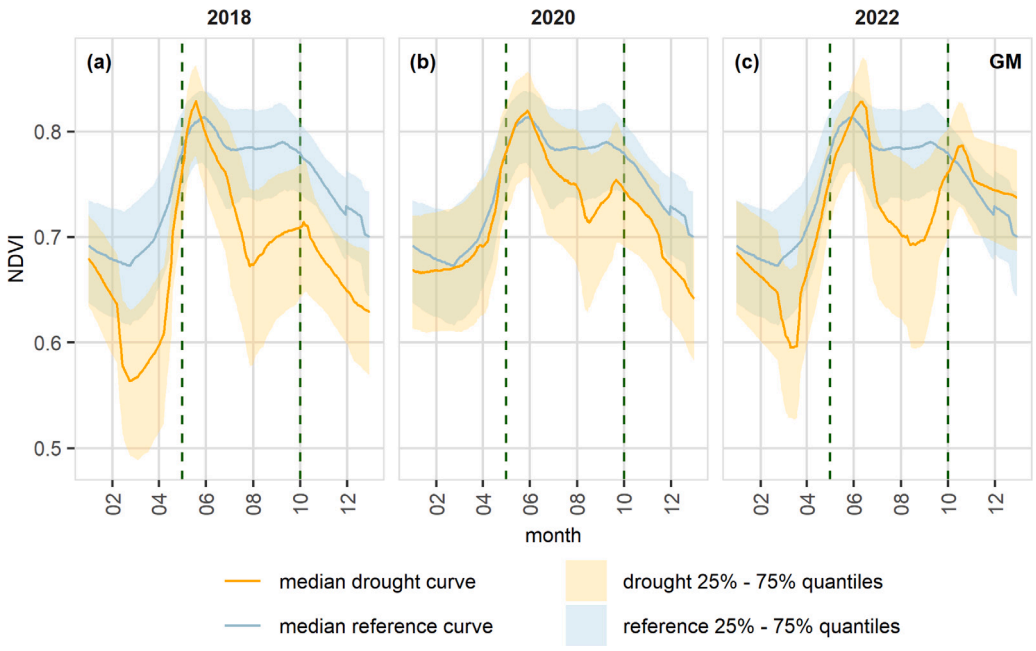

Fig. 4. Median reference curve and drought curves for the compounding hot and dry summers of 2018 (a), 2020 (b), and 2022 (c), calculated from the individual reference and drought curves of all "species-rich grasslands on fresh to moderately dry sites" (GM). Shaded areas represent the 25% and 75% quantiles. Green dashed lines indicate the vegetation green period from May 1 to September 30 used to compute mean NDVI differences between drought and reference curves. (For interpretation of the references to color in this figure legend, the reader is referred to the web version of this article.)

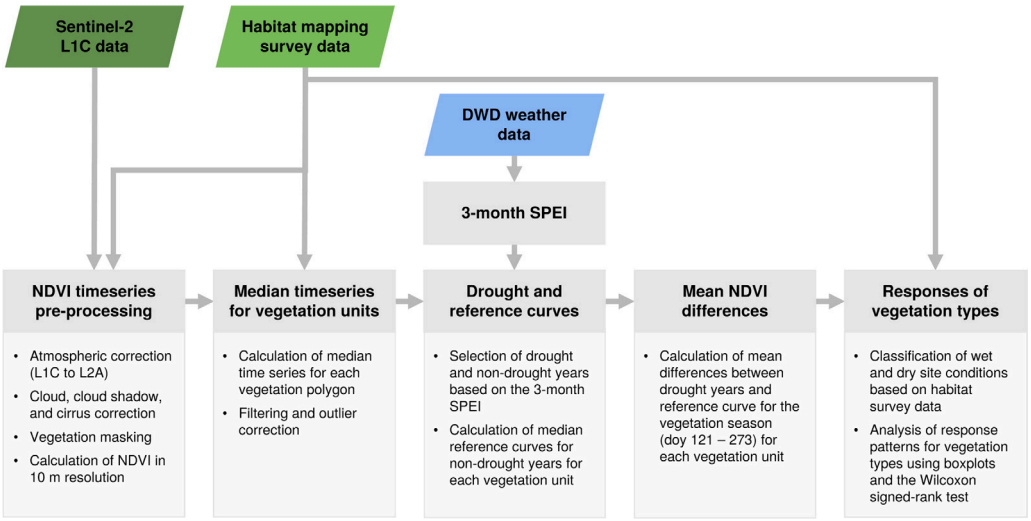

Fig. 5. Workflow illustrating the main data processing and analytical steps of the study and the associated datasets.

categories. Herbaceous vegetation in particular shows pronounced short-term responses to summer droughts, whereas woody vegetation appears unaffected in their NDVI. Among all vegetation types, grasslands display the most marked NDVI reductions during drought summers when compared to the reference curve (see Fig. 6). The deviation is particularly severe in the extreme summer of 2018, but significant for all years. Similarly, heathlands and dry grasslands, which are grouped together in one main vegetation cover category, show predominantly negative and significant deviations from the reference curves. Urban parks exhibit clear negative NDVI anomalies during the drought summer of 2018, too, while they appear less or even positively affected in 2020 and 2022, respectively.

By contrast, wetland vegetation types like swamps, fens and bogs do not show uniform NDVI deviations. While their NDVI deviations are statistically significant in all years, indicating drying in 2018 and 2020 and greening in 2022, their mean differences fluctuate around zero, indicating no systematic reduction in greenness during drought summers. Similarly, forests and shrublands do not show negative NDVI responses to summer droughts in the short-term. Instead, mean deviations are slightly positive and significant, implying greener canopies in drought years compared to the reference period. However, this apparent greening effect disappears when the vegetation period for computing the mean NDVI differences is adjusted to start on June 1st instead of May 1st (see Supplementary Material, Figure S4). When excluding May, most forests exhibit mean differences close to zero and shrubs even show negative deviations for 2018. In contrast to the general pattern, young afforestations are the only forest types that show pronounced reductions in NDVI in the drought summers of 2018 and 2020.

When looking into the NDVI deviations of the more detailed vegetation subgroups, the herbaceous and woody response patterns become

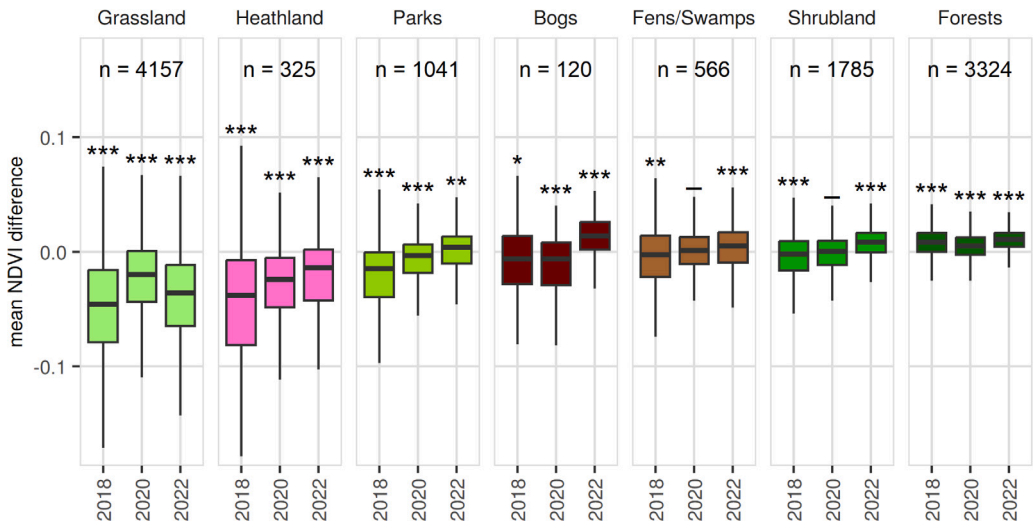

Fig. 6. Boxplots of mean NDVI differences for main vegetation cover categories in the three selected compounding hot and dry summers of 2018, 2020, and 2022, calculated as the mean deviation between each drought-year curve and the reference curve (May 1–September 30), with negative values indicating reduced greenness. Whiskers represent 1.5 x the interquartile range; outliers are omitted for clarity. Asterisks mark significant differences assessed via the non-parametric Wilcoxon signed-rank test (* $p < 0.05$, ** $p < 0.01$, *** $p < 0.001$).

more apparent (see Fig. 7 for 2018 and Supplementary Material, Figure S5 for 2020 and 2022). In vegetation cover categories that include herbaceous and woody vegetation types, like the heathland category that contains dry grasslands, the dry grasslands show responses like grasslands, with negative NDVI deviations in the drought summers, while dwarf-shrub heaths rather resemble the woody vegetation types with only very small deviations. Within the category of parks and cemeteries, tree-dominated types such as forest-like parks or forest cemeteries show only small deviations, whereas more herbaceous types respond with reductions in greenness during summer (see Supplementary Material, Figure S6). In correspondence with the negative deviations of young afforestations, the strongest negative responses are shown by new parks. Apart from these mixed herbaceous-woody vegetation categories, there are mostly no or rather weak differences in the responses of the subgroups within a category. Additionally, while woody vegetation types show only small variations in their NDVI deviations, herbaceous types differ much stronger in their reactions. As opposed to rather uniformly responding woody vegetation, herbaceous vegetation within a certain type reacts less consistent to summer droughts.

3.2. Responses of vegetation on wet and dry sites

By differentiating vegetation by site moisture conditions based on the habitat definitions, we find that for grasslands and heathlands, vegetation on dry sites exhibits stronger NDVI reductions than those classified as moist sites (see Fig. 8). This pattern can be further observed when looking at the NDVI differences of grasslands spatially (see Fig. 9). For 2018, we find that grassland vegetation in the higher-elevated north-western parts of Hamburg show stronger NDVI reductions than grasslands in the low-lying south-eastern marshlands (see Fig. 9(a)). This pattern is much less pronounced in 2020 and 2022 and not visible at all for forests and parks (see Supplementary Material, Figures S7, S8, S9), corresponding to the general lack of short-term responses in NDVI for these vegetation types. Nevertheless, we highlight a high spatial heterogeneity of responses for herbaceous vegetation, even in neighboring areas.

3.3. Strongest responses in the extreme summer of 2018

For the herbaceous vegetation types, the NDVI deviations are found to be higher in 2018 compared to 2020 and 2022, indicating that 2018 was the drought with the most severe ecological effects (see Figs. 6, 8). For most of the vegetation types, 2022 was least pronounced, with parks and bogs even exhibiting no or positive signals, respectively. Grasslands, however, show stronger negative deviations in 2022 than in 2020.

In summary, herbaceous vegetation types such as grasslands, heathlands, and parks exhibit notable phenological responsiveness to hot and dry summers, as indicated by negative NDVI anomalies. The response is especially pronounced on already dry sites. In contrast, woody and wetland vegetation types show either neutral or even positive NDVI deviations, suggesting limited short-term drought responsiveness detectable via the NDVI during the growing season.

4. Discussion

4.1. General response patterns correspond with large-scale studies

As demonstrated in the results, the vegetation in Hamburg does indeed respond to compounding hot and dry summers, and these responses vary considerably between vegetation types and at small spatial scales. The stronger responses of open, herbaceous vegetation to droughts on shorter time scales in contrast to forests correspond to findings in other larger-scale studies investigating the effects of hot droughts in recent years.

During the drought summer of 2018, pastures, arable land, and forests in regions with a negative climatic water balance were found to show lower than usual NDVI values, with a stronger relationship between climatic water balance and NDVI observed for pastures and arable land than for forests (Buras et al., 2020). Analyses of vegetation responses to the 2018 and 2019 droughts in Europe revealed stronger reactions for grassland and cropland compared to forests, which in contrast even exhibited greening effects (Bastos et al., 2021). Similarly, negative EVI (Enhanced Vegetation Index) anomalies were recorded for cropland and grasslands in 2018, while forests mainly showed positive anomalies and a pronounced greening in spring (Reinermann et al., 2019). These findings indicate that herbaceous vegetation often shows immediate responses to drought, whereas forests tend to react on longer timescales or with a temporal lag between the drought event and observable effects (Shyrokaya et al., 2024).

Similar drought response patterns have been reported across other climatic regions and drought events. Studies from Mediterranean and

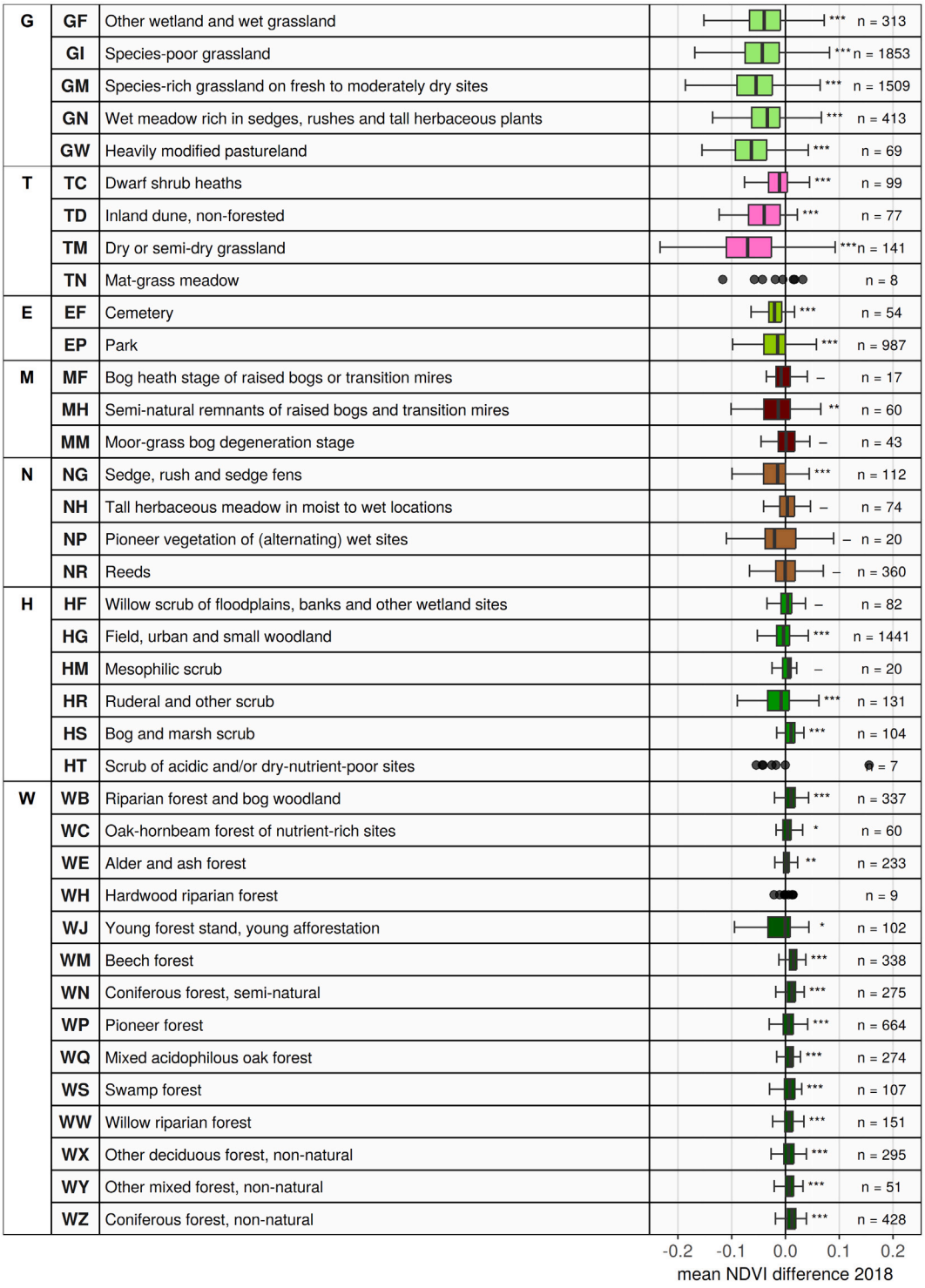

Fig. 7. Boxplots of mean NDVI differences for all vegetation subgroups in the compounding hot and dry summer of 2018, calculated as the mean deviation between each drought-year curve and the reference curve (May 1–September 30), with negative values indicating reduced greenness. Whiskers represent 1.5 x the interquartile range; outliers are omitted for clarity. Asterisks mark significant differences assessed via the non-parametric Wilcoxon signed-rank test (* $p < 0.05$, ** $p < 0.01$, *** $p < 0.001$). Abbreviations follow the German names of the vegetation types.

semi-arid urban environments consistently show that herbaceous vegetation responds more rapidly and more strongly to drought than woody vegetation. Analyses from California, based on both changes in green vegetation fractional cover (Allen et al., 2021) and NDVI–SPEI relationships (Miller et al., 2022), indicate that grasses are primarily sensitive to short-term drought conditions, whereas trees tend to exhibit delayed responses associated with longer-term moisture deficits. Similar contrasts between grasslands and forests have also been documented outside urban contexts, including the central United States (Gu et al., 2007), Southern China (Wu et al., 2024), and Spain (Vicente-Serrano et al., 2019). Across these regions, grasslands consistently exhibited stronger or earlier responses to short-term drought conditions, whereas forests tended to respond to longer SPEI time scales and showed

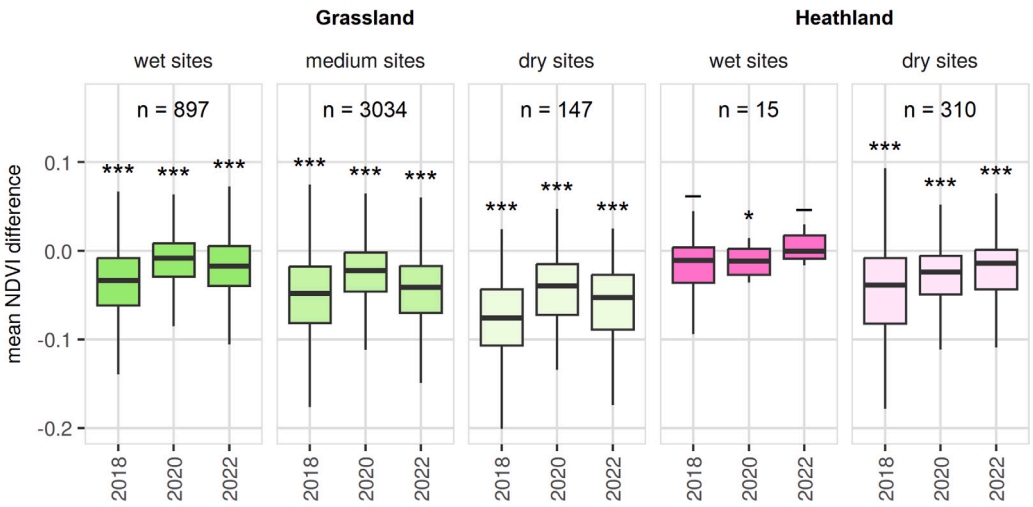

Fig. 8. Boxplots of mean NDVI differences for grasslands (G) and heathlands (T), classified according to their site conditions (wet, medium, dry), in the three selected compounding hot and dry summers of 2018, 2020, and 2022. Differences were calculated as the mean deviation between each drought-year curve and the reference curve (May 1–September 30), with negative values indicating reduced greenness. Whiskers represent 1.5 x the interquartile range; outliers are omitted for clarity. Asterisks mark significant differences assessed via the non-parametric Wilcoxon signed-rank test (* $p < 0.05$, ** $p < 0.01$, *** $p < 0.001$).

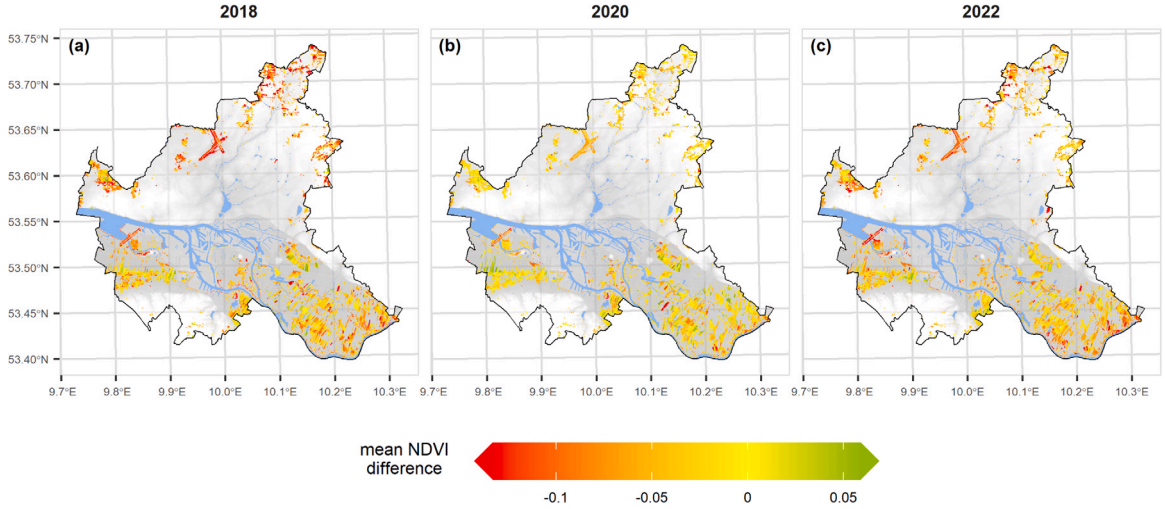

Fig. 9. Spatial distribution of mean NDVI differences for grasslands (G) during the hot and dry summers of (a) 2018, (b) 2020, and (c) 2022, calculated as the mean deviation between each drought-year curve and the reference curve (May 1–September 30), with negative values indicating reduced greenness. (For interpretation of the references to color in this figure legend, the reader is referred to the web version of this article.)

delayed but sustained reductions in greenness. The seasonal timing of drought responses can differ between regions. For example, in Mediterranean climates, NDVI declines during the typically dry summers are part of the normal seasonal cycle of annual grasslands, whereas unusual drought impacts are reflected in significant positive correlations between NDVI and SPEI during winter, when vegetation is typically active (Miller et al., 2022). Nevertheless, the underlying pattern remains consistent across continents and climate zones: herbaceous vegetation responds rapidly to water limitation, whereas woody vegetation shows more delayed and temporally buffered responses.

Although the general ecological response patterns observed in our study are consistent with these large-scale investigations, proving the robustness of our approach, our results reveal substantial fine-scale heterogeneity in vegetation responses, which can only be captured using high-resolution methods. Importantly, while vegetation types tend to follow characteristic response patterns, individual patches within the same type do not respond uniformly. Even in vegetation types that predominantly show reductions in NDVI, a substantial number of vegetation patches can show greening effects, and the magnitude of these responses vary markedly at small spatial scales. Moreover, spatially adjacent vegetation units may display contrasting reactions, and opposing responses between herbaceous and woody vegetation can compensate each other's signal if not assessed separately, potentially concealing important trends. Overall, our findings reveal a fine-scale mosaic of drought responses rather than homogeneous type-specific patterns, emphasizing the need for detailed, high-resolution monitoring and analysis of drought impact on vegetation to capture this variability.

4.2. Magnitude of drought response largely corresponds with drought intensity

Vegetation showing negative NDVI deviations during drought years mostly exhibited the strongest responses in 2018. The summer of 2018 stands out as the most extreme compounding hot and dry event in recent years, with negative SPEI values throughout the entire growing season (see Fig. 3). On a European scale, its impact on the vegetation even surpassed the extent of drought in the record summer of 2003 (Buras et al., 2020). In addition, the earlier spring greening due to

high spring temperatures (see Supplementary Material, Figure S10), as found by Reinermann et al. (2019) for vegetation in Germany in 2018, can lead to earlier soil water consumption and thus depletion, further intensifying the soil moisture drought in summer that occurred due to low precipitation and high temperatures (Wolf et al., 2016).

For most vegetation types, 2020 exhibited the second-strongest negative NDVI deviations, with the exception of grasslands, which showed stronger responses in 2022 (see Fig. 6). This indicates that the timing of the drought throughout the growing season may influence the response of the vegetation (Jin et al., 2023). In 2020 the meteorological drought reached its peak in May and June already with SPEI values below -1, and became less severe during summer with below average mean temperatures in July (Supplementary Material, Figure S10). In 2022, in contrast, the drought was comparably less severe in May and June, but stronger during July, August and September.

Additionally, the number of summer days with temperatures above 25°C was much higher for July in 2022 than in 2020 (Supplementary Material, Figure S11, DWD Climate Data Center, 2025c), which might have posed additional drought stress to grasslands, not only due to a raised evaporative demand due to higher temperatures, but due to the cooling strategy of herbaceous vegetation. In contrast to forests, herbaceous vegetation initially counters heat through increased evapotranspiration, providing evaporative cooling in the short term, but accelerating soil moisture depletion. Once reserves are exhausted, evapotranspiration cannot be maintained and the resulting shift in the Bowen ratio towards more sensible heat flux drives surface warming, further intensifying vegetation drying (Teuling et al., 2010). Heat can thus contribute to even faster soil moisture depletion due to enhanced evapotranspiration.

This enhanced drying of soil moisture due to vegetation activity is an effect that is not captured by meteorological drought indices like the SPEI. The magnitude of a soil moisture drought can thus be underestimated by such indices. A much higher number of hot days in July 2022 could be a factor explaining the stronger responses observed for grasslands during that summer than in 2020.

4.3. Herbaceous plants as indicators for small-scale differences in soil water availability and implications for urban climate

The three-month aggregated SPEI represents short-term meteorological droughts that primarily affect the uppermost soil layers, without necessarily extending into deeper soil layers or groundwater reserves (Ebeling et al., 2025). This explains why vegetation types composed of herbaceous plants with shallow root systems exhibit clear responses to the short-term hot and dry conditions, while trees with their deeper roots appear largely unaffected. The response patterns of herbaceous vegetation can therefore be used as indicator displaying in which areas soil moisture dropped below a tolerable level for herbaceous plants during the compounding hot and dry summers. This interpretation is supported by findings from West et al. (2018), who reported significant correlations between Sentinel-2-derived NDVI and soil moisture measured at 5–30 cm depth for grasslands in generally dry regions of the southwestern United States, demonstrating that NDVI of herbaceous vegetation can reliably reflect variations in near-surface soil moisture.

On sites where soil water is further limited by insufficient provision from the groundwater reserves, for instance, due to a low groundwater table or no hydraulic connectivity (Vogelbacher et al., 2024), soil moisture can be assumed to reach critical levels earlier, reducing the NDVI earlier during the drought and resulting in a higher mean deviance in NDVI. This is evident in the more pronounced responses observed in vegetation located on dry sites compared to those on wetter sites. On the contrary, vegetation that does not show a reduction in greenness during meteorological drought can be assumed to be supplied with sufficient water from groundwater reserves (Eamus et al., 2015; Graf et al., 2020), as indicated by the inconsistent responses of wetlands. But this does not necessarily imply that wetlands are less sensitive to drought. Instead, Northern European wetlands have shown to be highly sensitive (Jin et al., 2023), and the recurrence of droughts may pose a particular risk, as wet soils undergo biogeochemical changes due to drought that affect their ability to recover into the pre-drought state (Stirling et al., 2020). It may instead indicate that the short-term meteorological droughts investigated did not yet sufficiently alter the soil moisture regime in these systems in the investigated drought summers.

These spatial differences in soil moisture availability across the urban area are not only ecologically relevant but also have direct implications for urban climate regulation. Because the cooling capacity of herbaceous vegetation is directly linked to water availability, understanding spatial soil moisture regimes becomes essential for assessing where vegetation can effectively mitigate heat. While herbaceous vegetation accelerates evapotranspiration and thus the latent heat flux in the beginning of a heatwave, this function may collapse once soil moisture is depleted, contributing to local warming instead (Graf et al., 2020). In contrast, trees have been shown to maintain a measurable cooling effect even under severe drought conditions (e.g. Zandler and Samimi, 2024), particularly through shading beneath the canopy (Kraemer and Kabisch, 2022). Grasslands, however, exhibited markedly stronger reductions in cooling intensity, which was attributed to the higher drought sensitivity and more rapid desiccation of herbaceous vegetation (Allen et al., 2021). Together, these findings underline that the climatic function of urban green spaces during extreme events is strongly dependent on vegetation structure, rooting depth, and the ability to sustain evapotranspiration and shading under limited soil moisture availability during drought. In this context, the integration of optical satellite data with radar observations from Sentinel-1 offers considerable potential, as SAR-based information can support spatially explicit assessments of surface soil moisture and vegetation conditions independent of cloud cover (Dabrowska-Zielinska et al., 2017; Abdel-Hamid et al., 2020). Such combined approaches would enable a more comprehensive evaluation of hydrological constraints on urban vegetation and improve the identification of areas where cooling functions are most vulnerable during prolonged dry periods.

4.4. No immediate reductions in greenness for forests

In contrast to the herbaceous vegetation types, woody types like shrublands, dwarf shrub heaths, forests, and forest-like parks did not show negative NDVI deviations in the compounding hot and dry summers investigated, but instead exhibited positive deviations. Matching our findings, Reinermann et al. (2019) found positive EVI deviations for forests during 2018, with especially pronounced greening in April and May due to high spring temperatures. This early greening may help explain why positive NDVI deviations disappear when May is excluded from calculating the mean deviations (see Supplementary Material, Figure S4).

These results suggest that woody vegetation did not experience drought stress during the compounding hot and dry summers investigated, at least not to an extent causing reduced greenness. Unlike shallow-rooted herbaceous plants, trees can access, and even redistribute, water from deeper, wetter soil layers that are less affected by short-term meteorological droughts (Burgess et al., 1998). Furthermore, forests were found to not accelerate their evapotranspiration during hot days as much as grasslands, which inevitably leads to stronger heating in the crown region (Teuling et al., 2010). Due to this more conservative water-use strategy, forests do not additionally accelerate soil water depletion during hot days, but use water resources more sustainably (Teuling et al., 2010), which makes them less susceptible to short-term droughts that only affect the uppermost soil layers.

Shyrokaya et al. (2024) found that the number of drought impact reports for the forestry sector raised in 2019 compared to 2018, and found correlations only with longer SPI and SPEI time scales (12

and 24 months), indicating that longer SPEI time scales would be more suitable to represent drought for forests. In accordance, Vicente-Serrano et al. (2013) found that cool temperate moist forests show the highest correlations of the NDVI with intermediate SPEI time scales, whereas dry forests react to shorter time scales. However, even for a 12-month SPEI (see Supplementary Material, Figure S12), we did not find significant negative NDVI deviations in forests (see Supplementary Material, Figure S13).

Nevertheless, the lack of NDVI responses does not mean that forests have not been affected by drought during the compounding hot and dry summers. Instead, it implies that the water deficit was not causing hydraulic failure to an extent that would induce leaf abscission, crown defoliation or immediate mortality, which would result in a detectable reduction in their greenness (McDowell et al., 2022; Bréda et al., 2006; Carnicer et al., 2011). Nevertheless, Brun et al. (2020) found early-wilting for 11% of Central European forests in the hot and dry summer of 2018, and a tendency for reduced spring greening in 2019 in affected forests. This implies a reduction in foliage, and thus greening, during post-drought recovery after suffering xylem damage (Trugman et al., 2018). Accordingly, the only month Reinermann et al. (2019) found weak negative EVI anomalies (mean for Germany) for forests in 2018 was September, which might indicate an early-wilting effect, too. To investigate whether Hamburg's forests showed such a response, a more detailed phenological analysis would be necessary, since the pronounced greening in 2018 would have compensated an early-wilting signal in our analysis.

Furthermore, trees respond to moderate drought in physiological ways that are not immediately visible as a reduction in greenness. Isohydric species, for example, close their stomata when soil moisture becomes limited. This helps to avoid hydraulic failure, which can occur if evapotranspiration exceeds the critical water potential needed to maintain hydraulic conductance within the plant. While closing the stomata reduces water loss, it leads to reduced CO_2 uptake and thus reduced photosynthesis at the same time. Since the metabolic processes continue to demand carbohydrates, the plant will eventually starve if photosynthesis is limited to an amount that prevents replenishment of carbohydrate reserves (McDowell et al., 2008). Droughts can initiate this process of carbon starvation in different ways. Damages to the xylem structure of a tree due to severe drought can cause a tree to allocate more carbon into tree ring growth while neglecting the foliage, decreasing net plant productivity (Trugman et al., 2018). In addition or independently, moderate, but recurrent droughts as well as suboptimal growing conditions can continuously compromise the carbohydrate reserves of a tree until a critical threshold for inevitable mortality is reached (McDowell et al., 2022).

Moreover, while tree species differ in their water management strategies and adaptation to drought stress (Johnson et al., 2018; Bréda et al., 2006), even individuals within a species or population can show very different reactions to a drought, depending on, for example, individual traits like tree age, height, or individual differences in site factors that may cause chronic stresses, or competition between individuals (Trugman et al., 2021; Cailleret et al., 2017). Liu et al. (2022) demonstrated that drought reduced the annual shoot growth of younger trees, highlighting their higher sensitivity to water stress. This finding aligns with our observations of reduced greenness occurring primarily in young afforestations and recently planted parks. Moreover, trees growing within stands were found to exhibit weaker growth reductions than those growing individually along roads, underscoring the importance of microhabitat conditions in buffering drought effects (Liu et al., 2022). This may explain why smaller shrub and coppice vegetation units showed weak reductions in greenness (when excluding the spring greening effect, see Supplementary Material, Figure S4), while forests did not. Furthermore, trees growing on soils subject to the natural water cycle may be less susceptible to compounding hot and dry summers than, for example, street trees growing in artificial soil pits (Schütt et al., 2022; Leisenheimer et al., 2024), which were not part of this analysis. Therefore, by looking at whole vegetation units and by summarizing forest responses through median phenological curves, our analysis may have overlooked negative impacts on individual trees, especially such on unfavorable sites.

4.5. Methodological considerations and limitations

The agreement of our results with larger-scale and longer-term research proves the robustness of our overall results, despite the challenges and limitations posed by the much shorter available time series of Sentinel-2. Most notably, our analysis is restricted to short-term responses of vegetation and cannot assess long-term ecological trends or vegetation adaptations. Additionally, from the ten available years of data, we could only use seven due to the insufficient coverage of images in the first three years (see Fig. 2). The reference curves consist of four years and may therefore suffer from a low sample size.

Moreover, periods with higher precipitation are more likely to have clouds covering the area, reducing the number of usable images in comparison to dry years. The filtering procedure applied to remove outliers and smoothen the NDVI curves treats a time series as if the time steps were homogeneous (Granero-Belinchon et al., 2020). Therefore, it requires a sufficient number of available images per season to adequately reconstruct a phenological curve (Granero-Belinchon et al., 2021), which is not always the case. Large gaps or completely missing seasons therefore lead to a too strong smoothing of the time series, which can further underestimate the curves for wetter years (Granero-Belinchon et al., 2021).

Despite the challenges caused by the limited length of the time series, the high spatial resolution of Sentinel-2 data enables the investigation of drought patterns in small and fragmented urban vegetation, although varying sizes of vegetation units and their structural heterogeneity as well as differences in the available dates for each unit cause uncertainties in the reliability of the single time series. Firstly, vegetation units vary in size and are not fully homogeneous, meaning they mostly consist of mixed herbaceous and woody vegetation, each with different phenological behavior. By calculating the median for each unit and time step, we captured what a unit mostly consists of and reduced the influence of outliers. Nevertheless, when parts of a unit are missing in an image due to cloud cover, the proportion of herbaceous to woody vegetation can be distorted and influence the median of that date. However, this effect is partially accounted for by the smoothing procedure.

Secondly, the number of available dates and their distribution throughout the investigation period vary between vegetation units. Therefore, units that are closely located to each other can show different smoothing effects due to differing missing periods in their time series, and may therefore not be perfectly comparable. Additionally, and thirdly, there is the possibility of changes in land-use throughout the observation period. We used the newest habitat survey data available to attribute the vegetation types, but even over the short observation period, changes in land-use as well as in species composition of habitats (Lüttgert et al., 2022) may have occurred. Outlier patterns or stronger deviations in individual units could, therefore, stem from land-use changes or insufficient temporal representation rather than actual ecological responses. Nevertheless, the good correspondence of drought responses within vegetation cover categories supports the robustness of our results and highlights the suitability of the approach to investigate fine-scale drought responses in urban areas.

We employed the NDVI because it can be derived from Sentinel-2 bands at 10 m resolution and represents the most widely used vegetation index in remote sensing studies on drought monitoring (West et al., 2019), ensuring comparability across studies. Moreover, the spectral bands required for NDVI calculation are available on most satellite platforms and are commonly included in aerial imagery systems (Zhu et al., 2017; Olson and Anderson, 2021), further enhancing the transferability and operational applicability of the approach.

Nevertheless, there are many other indices that have been applied and tested for monitoring drought responses of vegetation, and especially to identify drought reactions of forests, it might be promising to employ vegetation indices that better represent multiple canopy layers (Huete, 2012) or the vegetation's water content, and to use an even finer spatial scale to capture individual tree responses. For example, indices employing short-wave infrared (SWIR) bands, such as the widely used NDWI (Normalized Difference Water Index, Gao, 1996), or the NDII (Kimes et al., 1981; Hardisky et al., 1983) and NBR (López García and Caselles, 1991; Key and Benson, 1999) that are more in correspondence to the Sentinel-2 SWIR bands (Ji et al., 2011), show a higher correlation with the plant water content of trees than the NDVI since the SWIR channel is especially sensitive to water (Marusig et al., 2020). A combination of the NDVI and NDWI (NDDI) was developed by Gu et al. (2007) and proved to be valuable for detecting drought in grasslands and cropland (Bartold et al., 2024; Dobri et al., 2021). Recent work has shown that several Sentinel-2-derived spectral indices, including NDII, correlate with chlorophyll fluorescence measurements in crop systems, even though chlorophyll fluorescence itself cannot be directly retrieved from Sentinel-2 data (Gurdak and Bartold, 2021). Because chlorophyll fluorescence is considered a highly sensitive indicator of physiological water stress (e.g. Banks, 2018), these findings further support the suitability of such indices for drought assessment and monitoring. Additionally, thermal indices have shown to be promising since they are able to detect changes in surface temperature of tree crowns due to reduced evapotranspiration (Le et al., 2023). Ultimately, investigating forest responses on pixel-scale might help to better identify responses of individual trees or tree groups without healthy trees compensating the signal of drought-stressed trees.

5. Conclusion

Our study demonstrates that short-term drought responses of vegetation cover types within the urban area of Hamburg vary both between vegetation types and at fine spatial scales. Herbaceous vegetation primarily exhibited declines in greenness during recent compounding hot and dry summers, whereas woody vegetation and wetlands remained rather unaffected.

Despite this overall pattern, we found that even within the same vegetation type, response magnitudes varied considerably across space, with some patches showing pronounced reductions while others remained relatively stable or even showed greening effects. This heterogeneity indicates that local drought responses are not uniform but are shaped by a complex interplay of species composition and site-specific factors, for example groundwater depth, elevation, soil type and structure, and the spatial distribution of precipitation.

Importantly, such fine-scale variation would remain undetected in coarser-resolution analyses, underscoring the value of high-resolution data for identifying localized vulnerabilities within seemingly homogeneous vegetation classes. By combining 10 m Sentinel-2 data with detailed in-situ vegetation type information from the habitat mapping survey, we were able to attribute drought responses to specific vegetation categories and uncover substantial heterogeneity within them.

At the same time, we highlight the potential of using herbaceous vegetation greenness, derived from NDVI, as indicator for remotely assessing near-surface soil moisture availability. The NDVI is one of the most widely applied indices in drought monitoring studies and can be consistently calculated from most other satellite platforms and even aerial imagery, which enhances the transferability of our methodological approach. Continuous monitoring or longer-term assessments based on this approach, or in combination with SAR-derived soil moisture data (Dabrowska-Zielinska et al., 2017; Abdel-Hamid et al., 2020), may therefore help identify climate change-related changes in hydrological conditions throughout the urban area of Hamburg and beyond.

Because NDVI-based approaches do not fully capture physiological stress responses in trees, forests in particular should be reassessed with complementary methods, such as thermal or physiological indicators and on finer spatial scale, to more accurately evaluate their drought sensitivity.

By providing one of the first systematic assessments of drought responses of urban vegetation in Northern Europe, our study begins to fill an important research gap. The spatially explicit response information could serve as a foundation for studies assessing the impact of drought on the vegetation's cooling capacity (Allen et al., 2021) or for multi-criteria decision analysis (MCDA, Łągiewska and Bartold, 2025) to support the prioritization of mitigation and adaptation measures in urban greening strategies.

Ultimately, fine-scale analyses are essential to identify areas within the urban landscape that are most at risk from drought or other environmental threats, which are projected to intensify under climate change. In the short term, assessing and monitoring the current vegetation state allows for immediate interventions on city scale, such as irrigation of parks or of ecologically valuable vegetation types. Over the long term, detailed analyses inform the development of adaptation strategies that account for the spatial heterogeneity of hydrological changes. In this way, targeted measures can be implemented to effectively preserve the ecosystem services provided by urban vegetation.

CRediT authorship contribution statement

Nadine Kaul: Writing – original draft, Visualization, Software, Methodology, Formal analysis, Data curation, Conceptualization. **Nikola Lenzewski:** Writing – review & editing, Supervision, Methodology. **Olaf Conrad:** Writing – review & editing, Software, Methodology. **Jürgen Böhner:** Writing – review & editing, Supervision, Funding acquisition, Conceptualization. **Kai Jensen:** Writing – review & editing, Supervision, Funding acquisition, Conceptualization. **Benjamin Poschlod:** Writing – review & editing, Supervision, Methodology, Conceptualization.

Declaration of Generative AI and AI-assisted technologies in the writing process

During the preparation of this work the authors used ChatGPT by OpenAI in order to conduct translations and improve grammar, sentence structure, and clarity. After using this tool/service, the authors reviewed and edited the content as needed and take full responsibility for the content of the published article.

Funding statement

This research is part of the project CLICCS C1: Sustainable Adaptation Scenarios for Urban Areas – "Water from Four Sides", funded by the Deutsche Forschungsgemeinschaft (DFG, German Research Foundation) under Germany's Excellence Strategy – EXC 2037 'CLICCS – Climate, Climatic Change, and Society' – Project Number: 390683824, contribution to the Center for Earth System Research and Sustainability (CEN) of Universität Hamburg.

Declaration of competing interest

The authors declare that they have no known competing financial interests or personal relationships that could have appeared to influence the work reported in this paper.

Acknowledgments

We thank Dr. Christoph Reisdorff for insightful discussions on tree physiology and drought responses, which substantially enhanced our understanding of drought-related processes in woody vegetation. We also gratefully acknowledge Samuel Heisterkamp for providing access to the most recent habitat mapping dataset, which was essential for carrying out the analyses presented here.

Appendix A. Supplementary data

Supplementary material related to this article can be found online at https://doi.org/10.1016/j.ufug.2026.129489.

Data availability

Hamburg Habitat NDVI Deviations During Compounding Hot and Dry Summers (Original data) (Mendeley Data)

References

Abdel-Hamid, A., Dubovyk, O., Graw, V., Greve, K., 2020. Assessing the impact of drought stress on grasslands using multi-temporal SAR data of Sentinel-1: a case study in Eastern Cape, South Africa. Eur. J. Remote. Sens. 53 (sup2), 3–16. http://dx.doi.org/10.1080/22797254.2020.1762514.

ACRI-ST, 2022. Sen2Cor 2.11.00 configuration and user manual: Issue 1.0, 21/11/2022. URL: https://step.esa.int/thirdparties/sen2cor/2.11.0/docs/OMPC.TPZG.SUM.001%20-%20i1r0%20-%20Sen2Cor%202.11.00%20Configuration%20and%20User%20Manual.pdf.

Allen, M.A., Roberts, D.A., McFadden, J.P., 2021. Reduced urban green cover and daytime cooling capacity during the 2012–2016 california drought. Urban Clim. 36, 100768. http://dx.doi.org/10.1016/j.uclim.2020.100768.

Banks, J.M., 2018. Chlorophyll fluorescence as a tool to identify drought stress in acer genotypes. Environ. Exp. Bot. 155, 118–127. http://dx.doi.org/10.1016/j.envexpbot.2018.06.022.

Bartold, M., Wróblewski, K., Kluczek, M., Dąbrowska-Zielińska, K., Goliński, P., 2024. Examining the sensitivity of satellite-derived vegetation indices to plant drought stress in grasslands in Poland. Plants (Basel, Switzerland) 13 (16), http://dx.doi.org/10.3390/plants13162319.

Bastos, A., Ciais, P., Friedlingstein, P., Sitch, S., Pongratz, J., Fan, L., Wigneron, J.P., Weber, U., Reichstein, M., Fu, Z., Anthoni, P., Arneth, A., Haverd, V., Jain, A.K., Joetzjer, E., Knauer, J., Lienert, S., Loughran, T., McGuire, P.C., Tian, H., Viovy, N., Zaehle, S., 2020. Direct and seasonal legacy effects of the 2018 heat wave and drought on European ecosystem productivity. Sci. Adv. 6 (24), eaba2724. http://dx.doi.org/10.1126/sciadv.aba2724.

Bastos, A., Orth, R., Reichstein, M., Ciais, P., Viovy, N., Zaehle, S., Anthoni, P., Arneth, A., Gentine, P., Joetzjer, E., Lienert, S., Loughran, T., McGuire, P.C., O, S., Pongratz, J., Sitch, S., 2021. Vulnerability of European ecosystems to two compound dry and hot summers in 2018 and 2019. Earth Syst. Dyn. 12 (4), 1015–1035. http://dx.doi.org/10.5194/esd-12-1015-2021.

Beguería, S., Vicente-Serrano, S.M., 2023. SPEI: Calculation of the standardized precipitation-evapotranspiration index. URL: https://CRAN.R-project.org/package=SPEI R package version 1.8.1.

Böhnisch, A., Felsche, E., Mittermeier, M., Poschlod, B., Ludwig, R., 2025. Future patterns of compound dry and hot summers and their link to soil moisture droughts in europe. Earth's Futur. 13 (2), e2024EF004916. http://dx.doi.org/10.1029/2024EF004916.

Brandt, I., Haacks, M., Hastedt, J., Heisterkamp, S., Michalczyk, C., Schulze, D., 2025. Kartieranleitung und Biotoptypenschlüssel für die Biotopkartierung in Hamburg: einschließlich der Definitionen besonders geschützter Biotope nach § 30 BNatSchG in Verbindung mit § 14 HmbBNatSchAG und unter Berücksichtigung der Lebensraumtypen gemäßFH-Richtlinie der EU, 7. überarbeitete Auflage, Stand März 2025 Freie und Hansestadt Hamburg, Behörde für Umwelt, Klima, Energie und Agrarwirtschaft, Hamburg, URL: https://www.hamburg.de/resource/blob/1036252/de53ab36043c5d658b46aa8d4337c97b/kartieranleitung-biotoptypenschluessel-maerz-2025-data.pdf.

Brás, T.A., Seixas, J., Carvalhais, N., Jägermeyr, J., 2021. Severity of drought and heatwave crop losses tripled over the last five decades in europe. Environ. Res. Lett. 16 (6), 065012. http://dx.doi.org/10.1088/1748-9326/abf004.

Bréda, N., Huc, R., Granier, A., Dreyer, E., 2006. Temperate forest trees and stands under severe drought: a review of ecophysiological responses, adaptation processes and long-term consequences. Ann. For. Sci. 63 (6), 625–644. http://dx.doi.org/10.1051/forest:2006042.

Brun, P., Psomas, A., Ginzler, C., Thuiller, W., Zappa, M., Zimmermann, N.E., 2020. Large-scale early-wilting response of central European forests to the 2018 extreme drought. Global Change Biol. 26 (12), 7021–7035. http://dx.doi.org/10.1111/gcb.15360.

Buras, A., Rammig, A., Zang, C.S., 2020. Quantifying impacts of the 2018 drought on European ecosystems in comparison to 2003. Biogeosciences 17 (6), 1655–1672. http://dx.doi.org/10.5194/bg-17-1655-2020.

Burgess, S.S.O., Adams, M.A., Turner, N.C., Ong, C.K., 1998. The redistribution of soil water by tree root systems. Oecologia 115 (3), 306–311. http://dx.doi.org/10.1007/s004420050521.

Cailleret, M., Jansen, S., Robert, E.M.R., Desoto, L., Aakala, T., Antos, J.A., Beikircher, B., Bigler, C., Bugmann, H., Caccianiga, M., Čada, V., Camarero, J.J., Cherubini, P., Cochard, H., Coyea, M.R., Čufar, K., Das, A.J., Davi, H., Delzon, S., Dorman, M., Gea-Izquierdo, G., Gillner, S., Haavik, L.J., Hartmann, H., Hereş, A.-M., Hultine, K.R., Janda, P., Kane, J.M., Kharuk, V.I., Kitzberger, T., Klein, T., Kramer, K., Lens, F., Levanic, T., Linares Calderon, J.C., Lloret, F., Lobo-Do-Vale, R., Lombardi, F., López Rodríguez, R., Mäkinen, H., Mayr, S., Mészáros, I., Metsaranta, J.M., Minunno, F., Oberhuber, W., Papadopoulos, A., Peltoniemi, M., Petritan, A.M., Rohner, B., Sangüesa-Barreda, G., Sarris, D., Smith, J.M., Stan, A.B., Sterck, F., Stojanović, D.B., Suarez, M.L., Svoboda, M., Tognetti, R., Torres-Ruiz, J.M., Trotsiuk, V., Villalba, R., Vodde, F., Westwood, A.R., Wyckoff, P.H., Zafirov, N., Martínez-Vilalta, J., 2017. A synthesis of radial growth patterns preceding tree mortality. Global Change Biol. 23 (4), 1675–1690. http://dx.doi.org/10.1111/gcb.13535.

Carnicer, J., Coll, M., Ninyerola, M., Pons, X., Sánchez, G., Peñuelas, J., 2011. Widespread crown condition decline, food web disruption, and amplified tree mortality with increased climate change-type drought. Proc. Natl. Acad. Sci. USA 108 (4), 1474–1478. http://dx.doi.org/10.1073/pnas.1010070108.

Chen, J., Jönsson, P., Tamura, M., Gu, Z., Matsushita, B., Eklundh, L., 2004. A simple method for reconstructing a high-quality NDVI time-series data set based on the Savitzky–Golay filter. Remote Sens. Environ. 91 (3–4), 332–344. http://dx.doi.org/10.1016/j.rse.2004.03.014.

Christidis, N., Jones, G.S., Stott, P.A., 2015. Dramatically increasing chance of extremely hot summers since the 2003 European heatwave. Nat. Clim. Chang. 5 (1), 46–50. http://dx.doi.org/10.1038/nclimate2468.

Ciais, P., Reichstein, M., Viovy, N., Granier, A., Ogée, J., Allard, V., Aubinet, M., Buchmann, N., Bernhofer, C., Carrara, A., Chevallier, F., de Noblet, N., Friend, A.D., Friedlingstein, P., Grünwald, T., Heinesch, B., Keronen, P., Knohl, A., Krinner, G., Loustau, D., Manca, G., Matteucci, G., Miglietta, F., Ourcival, J.M., Papale, D., Pilegaard, K., Rambal, S., Seufert, G., Soussana, J.F., Sanz, M.J., Schulze, E.D., Vesala, T., Valentini, R., 2005. Europe-wide reduction in primary productivity caused by the heat and drought in 2003. Nature 437 (7058), 529–533. http://dx.doi.org/10.1038/nature03972.

Conrad, O., Bechtel, B., Bock, M., Dietrich, H., Fischer, E., Gerlitz, L., Wehberg, J., Wichmann, V., Böhner, J., 2015. System for Automated Geoscientific Analyses (SAGA) v. 2.1.4. Geosci. Model. Dev. 8 (7), 1991–2007. http://dx.doi.org/10.5194/gmd-8-1991-2015.

Copernicus, 2023. Copernicus DEM - global and European digital elevation model - GLO-30 [dataset]. http://dx.doi.org/10.5270/ESA-c5d3d65, Downloaded on: 25.09.2023.

Copernicus Data Space Ecosystem, 2025. [Online]. URL: https://dataspace.copernicus.eu/browser/ Last (Accessed 12 November 2025).

Crausbay, S.D., Ramirez, A.R., Carter, S.L., Cross, M.S., Hall, K.R., Bathke, D.J., Betancourt, J.L., Colt, S., Cravens, A.E., Dalton, M.S., Dunham, J.B., Hay, L.E., Hayes, M.J., McEvoy, J., McNutt, C.A., Moritz, M.A., Nislow, K.H., Raheem, N., Sanford, T., 2017. Defining Ecological Drought for the Twenty-First Century. Bull. Am. Meteorol. Soc. 98 (12), 2543–2550. http://dx.doi.org/10.1175/BAMS-D-16-0292.1.

Dabrowska-Zielinska, K., Bochenek, Z., Malinska, A., Bartold, M., Gurdak, R., Lagiewska, M., Paradowski, K., 2021. Drought assessment applying joined meteorological and satellite data. In: 2021 IEEE International Geoscience and Remote Sensing Symposium IGARSS. pp. 6591–6594. http://dx.doi.org/10.1109/IGARSS47720.2021.9553739.

Dabrowska-Zielinska, K., Budzynska, M., Gurdak, R., Musial, J., Malinska, A., Gatkowska, M., Bartold, M., 2017. Application of sentinel-1 VH and VV and sentinel-2 for soil moisture studies. In: Notarnicola, C., Pierdicca, N., Santi, E. (Eds.), Active and Passive Microwave Remote Sensing for Environmental Monitoring. In: Proc. SPIE, SPIE, p. 13. http://dx.doi.org/10.1117/12.2278613.

Dabrowska-Zielinska, K., Malinska, A., Bochenek, Z., Bartold, M., Gurdak, R., Paradowski, K., Lagiewska, M., 2020. Drought model DISS based on the fusion of satellite and meteorological data under variable climatic conditions. Remote. Sens. 12 (18), 2944. http://dx.doi.org/10.3390/rs12182944.

Defourny, P., Lamarche, C., Bontemps, S., de Maet, T., van Bogaert, E., Moreau, I., Brockmann, C., Boettcher, M., Kirches, G., Wevers, J., Santoro, M., Ramoino, F., Arino, O., 2017. Land cover climate change initiative - product user guide v2. Issue 2.0.. URL: http://maps.elie.ucl.ac.be/CCI/viewer/download/ESACCI-LC-Ph2-PUGv2_2.0.pdf last (Accessed: 16 August 2025).

Deutscher Wetterdienst, 2023/2024. Vieljährige Mittelwerte. URL: https://www.dwd.de/DE/leistungen/klimadatendeutschland/vielj_mittelwerte.html (Accessed: 13 February 2025).

Dobri, R.-V., Sfîcă, L., Amihăesei, V.-A., Apostol, L., Tîmpu, S., 2021. Drought extent and severity on arable lands in Romania derived from normalized difference drought index (2001–2020). Remote. Sens. 13 (8), 1478. http://dx.doi.org/10.3390/rs13081478.

DWD Climate Data Center, 2025a. Monthly station observations (temperature, precipitation, sunshine duration, wind and cloud cover) for Germany, version v24.03. URL: https://opendata.dwd.de/climate_environment/CDC/observations_germany/climate/monthly/kl/ (Accessed: 04 April 2025).

DWD Climate Data Center, 2025b. Calculated monthly values for different characteristic elements of soil and crops, version v19.3, 2019. URL: https://opendata.dwd.de/climate_environment/CDC/derived_germany/soil/monthly/ (Accessed: 04 February 2025).

DWD Climate Data Center, 2025c. Monthly climatic indices (ice days, frost days, hot days, summer days, tropical nights) for Germany. URL: https://opendata.dwd.de/climate_environment/CDC/observations_germany/climate/monthly/climate_indices/kl/ (Accessed: 04 February 2025).

Eamus, D., Zolfaghar, S., Villalobos-Vega, R., Cleverly, J., Huete, A., 2015. Groundwater-dependent ecosystems: recent insights from satellite and field-based studies. Hydrol. Earth Syst. Sci. 19 (10), 4229–4256. http://dx.doi.org/10.5194/hess-19-4229-2015.

Ebeling, P., Musolff, A., Kumar, R., Hartmann, A., Fleckenstein, J.H., 2025. Groundwater head responses to droughts across Germany. Hydrol. Earth Syst. Sci. 29 (13), 2925–2950. http://dx.doi.org/10.5194/hess-29-2925-2025.

Felsche, E., Böhnisch, A., Poschlod, B., Ludwig, R., 2024. European hot and dry summers are projected to become more frequent and expand northwards. Commun. Earth & Environ. 5 (1), http://dx.doi.org/10.1038/s43247-024-01575-5.

Fu, Z., Ciais, P., Prentice, I.C., Gentine, P., Makowski, D., Bastos, A., Luo, X., Green, J.K., Stoy, P.C., Yang, H., Hajima, T., 2022. Atmospheric dryness reduces photosynthesis along a large range of soil water deficits. Nat. Commun. 13 (1), 989. http://dx.doi.org/10.1038/s41467-022-28652-7.

Gampe, D., Zscheischler, J., Reichstein, M., O'Sullivan, M., Smith, W.K., Sitch, S., Buermann, W., 2021. Increasing impact of warm droughts on northern ecosystem productivity over recent decades. Nat. Clim. Chang. 11 (9), 772–779. http://dx.doi.org/10.1038/s41558-021-01112-8.

Gao, B.-c., 1996. NDWI - a normalized difference water index for remote sensing of vegetation liquid water from space. Remote Sens. Environ. 58 (3), 257–266. http://dx.doi.org/10.1016/S0034-4257(96)00067-3.

García-Herrera, R., Díaz, J., Trigo, R.M., Luterbacher, J., and, E.M.F., 2010. A review of the European summer heat wave of 2003. Crit. Rev. Environ. Sci. Technol. 40 (4), 267–306. http://dx.doi.org/10.1080/10643380802238137.

García-León, D., Casanueva, A., Standardi, G., Burgstall, A., Flouris, A.D., Nybo, L., 2021. Current and projected regional economic impacts of heatwaves in europe. Nat. Commun. 12 (1), 5807. http://dx.doi.org/10.1038/s41467-021-26050-z.

Graf, A., Klosterhalfen, A., Arriga, N., Bernhofer, C., Bogena, H., Bornet, F., Brüggemann, N., Brümmer, C., Buchmann, N., Chi, J., Chipeaux, C., Cremonese, E., Cuntz, M., Dušek, J., El-Madany, T.S., Fares, S., Fischer, M., Foltýnová, L., Gharun, M., Ghiasi, S., Gielen, B., Gottschalk, P., Grünwald, T., Heinemann, G., Heinesch, B., Heliasz, M., Holst, J., Hörtnagl, L., Ibrom, A., Ingwersen, J., Jurasinski, G., Klatt, J., Knohl, A., Koebsch, F., Konopka, J., Korkiakoski, M., Kowalska, N., Kremer, P., Kruijt, B., Lafont, S., Léonard, J., de Ligne, A., Longdoz, B., Loustau, D., Magliulo, V., Mammarella, I., Manca, G., Mauder, M., Migliavacca, M., Mölder, M., Neirynck, J., Ney, P., Nilsson, M., Paul-Limoges, E., Peichl, M., Pitacco, A., Poyda, A., Rebmann, C., Roland, M., Sachs, T., Schmidt, M., Schrader, F., Siebicke, L., Šigut, L., Tuittila, E.-S., Varlagin, A., Vendrame, N., Vincke, C., Völksch, I., Weber, S., Wille, C., Wizemann, H.-D., Zeeman, M., Vereecken, H., 2020. Altered energy partitioning across terrestrial ecosystems in the European drought year 2018. Philos. Trans. R. Soc. Lond. Ser. B, Biol. Sci. 375 (1810), 20190524. http://dx.doi.org/10.1098/rstb.2019.0524.

Granero-Belinchon, C., Adeline, K., Briottet, X., 2021. Impact of the number of dates and their sampling on a NDVI time series reconstruction methodology to monitor urban trees with venμs satellite. Int. J. Appl. Earth Obs. Geoinf. 95, 102257. http://dx.doi.org/10.1016/j.jag.2020.102257.

Granero-Belinchon, C., Adeline, K., Lemonsu, A., Briottet, X., 2020. Phenological dynamics characterization of alignment trees with sentinel-2 imagery: A vegetation indices time series reconstruction methodology adapted to urban areas. Remote. Sens. 12 (4), 639. http://dx.doi.org/10.3390/rs12040639.

Gu, Y., Brown, J.F., Verdin, J.P., Wardlow, B., 2007. A five–year analysis of MODIS NDVI and NDWI for grassland drought assessment over the central great plains of the United States. Geophys. Res. Lett. 34 (6), http://dx.doi.org/10.1029/2006GL029127.

Guidolotti, G., Zenone, T., Endreny, T., Pace, R., Ciolfi, M., Mattioni, M., Pallozzi, E., Rezaie, N., Bertolini, T., Corradi, C., Calfapietra, C., 2025. Impact of drought on cooling capacity and carbon sequestration in urban green area. Urban Clim. 59, 102244. http://dx.doi.org/10.1016/j.uclim.2024.102244.

Gurdak, R., Bartold, M., 2021. Remote sensing techniques to assess chlorophyll fluorescence in support of crop monitoring in Poland. Misc. Geogr. 25 (4), 226–237. http://dx.doi.org/10.2478/mgrsd-2020-0029.

Hanf, F.S., Ament, F., Boettcher, M., Burgemeister, F., Gaslikova, L., Hoffmann, P., Knieling, J., Matthias, V., Meier, L., Pein, J., Poschlod, B., Quante, M., Ratzke, L., Rudolph, E., Scheffran, J., Schlünzen, K.H., Shokri, N., Sillmann, J., Vogelbacher, A., von Szombathely, M., Wickel, M., 2025. Towards a socio-ecological system understanding of urban flood risk and barriers to climate change adaptation using causal loop diagrams. Int. J. Urban Sustain. Dev. 17 (1), 69–102. http://dx.doi.org/10.1080/19463138.2025.2474399.

Hardisky, M.A., Klemas, V., Smart, R.M., 1983. The influence of soil salinity, growth form, and leaf moisture on-the spectral radiance of spartina alterniflora canopies. Photogramm. Eng. Remote Sens. 49, 77–83.

Huete, A.R., 2012. Vegetation indices, remote sensing and forest monitoring. Geogr. Compass 6 (9), 513–532. http://dx.doi.org/10.1111/j.1749-8198.2012.00507.x.

Ji, L., Zhang, L., Wylie, B.K., Rover, J., 2011. On the terminology of the spectral vegetation index (NIR − SWIR)/(NIR + SWIR). Int. J. Remote Sens. 32 (21), 6901–6909. http://dx.doi.org/10.1080/01431161.2010.510811.

Jin, H., Vicente-Serrano, S.M., Tian, F., Cai, Z., Conradt, T., Boincean, B., Murphy, C., Farizo, B.A., Grainger, S., López-Moreno, J.I., Eklundh, L., 2023. Higher vegetation sensitivity to meteorological drought in autumn than spring across European biomes. Commun. Earth & Environ. 4 (1), http://dx.doi.org/10.1038/s43247-023-00960-w.

Johnson, D.M., Domec, J.-C., Carter Berry, Z., Schwantes, A.M., McCulloh, K.A., Woodruff, D.R., Wayne Polley, H., Wortemann, R., Swenson, J.J., Scott Mackay, D., McDowell, N.G., Jackson, R.B., 2018. Co-occurring woody species have diverse hydraulic strategies and mortality rates during an extreme drought. Plant, Cell & Environ. 41 (3), 576–588. http://dx.doi.org/10.1111/pce.13121.

Kabisch, N., Kraemer, R., Brenck, M.E., Haase, D., Lausch, A., Luttkus, M.L., Mueller, T., Remmler, P., von Döhren, P., Voigtländer, J., Bumberger, J., 2021. A methodological framework for the assessment of regulating and recreational ecosystem services in urban parks under heat and drought conditions. Ecosyst. People 17 (1), 464–475. http://dx.doi.org/10.1080/26395916.2021.1958062.

Key, C.H., Benson, N.C., 1999. Measuring and remote sensing of burn severity: the CBI and NBR. In: Neuenschwander, L.F., Ryan, K.C. (Eds.), Proceedings Joint Fire Science Conference and Workshop, Vol. II, Boise, ID, 15-17 June 1999, University of Idaho and International Association of Wildland Fire.

Kimes, D., Markham, B., Tucker, C., McMurtrey, J., 1981. Temporal relationships between spectral response and agronomic variables of a corn canopy. Remote Sens. Environ. 11, 401–411. http://dx.doi.org/10.1016/0034-4257(81)90037-7.

King, A.D., Black, M.T., Min, S.-K., Fischer, E.M., Mitchell, D.M., Harrington, L.J., Perkins-Kirkpatrick, S.E., 2016. Emergence of heat extremes attributable to anthropogenic influences. Geophys. Res. Lett. 43 (7), 3438–3443. http://dx.doi.org/10.1002/2015GL067448.

Kraemer, R., Kabisch, N., 2022. Parks under stress: Air temperature regulation of urban green spaces under conditions of drought and summer heat. Front. Environ. Sci. 10, http://dx.doi.org/10.3389/fenvs.2022.849965.

Łągiewska, M., Bartold, M., 2025. An integrated approach using remote sensing and multi-criteria decision analysis to mitigate agricultural drought impact in the Mazowieckie Voivodeship, Poland. Remote. Sens. 17 (7), 1158. http://dx.doi.org/10.3390/rs17071158.

Lawler, J., Enquist, C., Girvetz, E., 2011. Assessing the components of vulnerability. In: Glick, P., Stein, B.A., Edelson, N.A. (Eds.), Scanning the Conservation Horizon: A Guide To Climate Change Vulnerability Assessment. National Wildlife Federation, Washington, D.C., pp. 39–50.

Le, T.S., Harper, R., Dell, B., 2023. Application of remote sensing in detecting and monitoring water stress in forests. Remote. Sens. 15 (13), 3360. http://dx.doi.org/10.3390/rs15133360.

Le Saint, T., Nabucet, J., Michéa, D., Hubert-Moy, L., Adeline, K., 2026. Assessing effects of drought and urbanization on urban trees using sentinel-2 time series. IEEE J. Sel. Top. Appl. Earth Obs. Remote. Sens. 19, 6290–6312. http://dx.doi.org/10.1109/JSTARS.2026.3656699.

Leisenheimer, L., Wellmann, T., Jänicke, C., Haase, D., 2024. Monitoring drought impacts on street trees using remote sensing - Disentangling temporal and species-specific response patterns with Sentinel-2 imagery. Ecol. Inform. 82, 102659. http://dx.doi.org/10.1016/j.ecoinf.2024.102659.

Liu, M., Pietzarka, U., Meyer, M., Kniesel, B., Roloff, A., 2022. Annual shoot length of temperate broadleaf species responses to drought. Urban For. & Urban Green. 73, 127592. http://dx.doi.org/10.1016/j.ufug.2022.127592.

López García, M.J., Caselles, V., 1991. Mapping burns and natural reforestation using thematic Mapper data. Geocarto Int. 6 (1), 31–37. http://dx.doi.org/10.1080/10106049109354290.

Lüttgert, L., Heisterkamp, S., Jansen, F., Klenke, R., Kreft, K.-A., Seidler, G., Bruelheide, H., 2022. Repeated habitat mapping data reveal gains and losses of plant species. Ecosphere 13 (10), http://dx.doi.org/10.1002/ecs2.4244.

Mangiafico, S.S., 2026. rcompanion: Functions to support extension education program evaluation. URL: https://CRAN.R-project.org/package=rcompanion/ version 2.5.2.

Markonis, Y., Kumar, R., Hanel, M., Rakovec, O., Máca, P., AghaKouchak, A., 2021. The rise of compound warm-season droughts in Europe. Sci. Adv. 7 (6), http://dx.doi.org/10.1126/sciadv.abb9668.

Marusig, D., Petruzzellis, F., Tomasella, M., Napolitano, R., Altobelli, A., Nardini, A., 2020. Correlation of field-measured and remotely sensed plant water status as a tool to monitor the risk of drought-induced forest decline. Forests 11 (1), 77. http://dx.doi.org/10.3390/f11010077.

McDowell, N., Pockman, W.T., Allen, C.D., Breshears, D.D., Cobb, N., Kolb, T., Plaut, J., Sperry, J., West, A., Williams, D.G., Yepez, E.A., 2008. Mechanisms of plant survival and mortality during drought: why do some plants survive while others succumb to drought? New Phytol. 178 (4), 719–739. http://dx.doi.org/10.1111/j.1469-8137.2008.02436.x.

McDowell, N.G., Sapes, G., Pivovaroff, A., Adams, H.D., Allen, C.D., Anderegg, W.R.L., Arend, M., Breshears, D.D., Brodribb, T., Choat, B., Cochard, H., de Cáceres, M., de Kauwe, M.G., Grossiord, C., Hammond, W.M., Hartmann, H., Hoch, G., Kahmen, A., Klein, T., Mackay, D.S., Mantova, M., Martínez-Vilalta, J., Medlyn, B.E., Mencuccini, M., Nardini, A., Oliveira, R.S., Sala, A., Tissue, D.T., Torres-Ruiz, J.M., Trowbridge, A.M., Trugman, A.T., Wiley, E., Xu, C., 2022. Mechanisms of woody-plant mortality under rising drought, CO2 and vapour pressure deficit. Nat. Rev. Earth & Environ. 3 (5), 294–308. http://dx.doi.org/10.1038/s43017-022-00272-1.

McKee, T.B., Doesken, N.J., Kleist, J., 1993. The relationship of drought frequency and duration to time scales. In: Eighth Conference on Applied Climatology 17 - 22 January 1993.

McMahon, C.A., Roberts, D.A., Stella, J.C., Trugman, A.T., Singer, M.B., Caylor, K.K., 2024. A river runs through it: Robust automated mapping of riparian woodlands and land surface phenology across dryland regions. Remote Sens. Environ. 305, 114056. http://dx.doi.org/10.1016/j.rse.2024.114056.

Miller, D.L., Alonzo, M., Meerdink, S.K., Allen, M.A., Tague, C.L., Roberts, D.A., McFadden, J.P., 2022. Seasonal and interannual drought responses of vegetation in a California urbanized area measured using complementary remote sensing indices. ISPRS J. Photogramm. Remote Sens. 183, 178–195. http://dx.doi.org/10.1016/j.isprsjprs.2021.11.002.

Ministry for Environment, Climate, Energy and Agriculture, 2024. Biotopkataster Hamburg. Freie und Hansestadt Hamburg, Behörde für Umwelt, Klima, Energie und Agrarwirtschaft (BUKEA), URL: https://metaver.de/trefferanzeige?docuuid=D7B5CCBB-1F03-4482-AB59-26F2F7972547.

Monteith, J.L., 1965. Evaporation and environment. Symp. Soc. Exp. Biology 19, 205–234, URL: https://repository.rothamsted.ac.uk/item/8v5v7/evaporation-and-environment.

Olson, D., Anderson, J., 2021. Review on unmanned aerial vehicles, remote sensors, imagery processing, and their applications in agriculture. Agron. J. 113 (2), 971–992. http://dx.doi.org/10.1002/agj2.20595.

Qiu, S., Zhu, Z., He, B., 2019. Fmask 4.0: Improved cloud and cloud shadow detection in landsats 4–8 and sentinel-2 imagery. Remote Sens. Environ. 231, 111205. http://dx.doi.org/10.1016/j.rse.2019.05.024.

R Core Team, 2025. R: A Language and Environment for Statistical Computing. R Foundation for Statistical Computing, Vienna, Austria, URL: https://www.R-project.org/.

Reinermann, S., Gessner, U., Asam, S., Kuenzer, C., Dech, S., 2019. The Effect of Droughts on Vegetation Condition in Germany: An Analysis Based on Two Decades of Satellite Earth Observation Time Series and Crop Yield Statistics. Remote. Sens. 11 (15), 1783. http://dx.doi.org/10.3390/rs11151783.

Robine, J.-M., Cheung, S.L.K., Le Roy, S., van Oyen, H., Griffiths, C., Michel, J.-P., Herrmann, F.R., 2008. Death toll exceeded 70,000 in Europe during the summer of 2003. Comptes Rendus Biologies 331 (2), 171–178. http://dx.doi.org/10.1016/j.crvi.2007.12.001.

Rohat, G., Goyette, S., Flacke, J., 2017. Twin climate cities – an exploratory study of their potential use for awareness-raising and urban adaptation. Mitig. Adapt. Strat. Glob. Chang. 22 (6), 929–945. http://dx.doi.org/10.1007/s11027-016-9708-x.

Roshani, Sajjad, H., Kumar, P., Masroor, M., Rahaman, M.H., Rehman, S., Ahmed, R., Sahana, M., 2022. Forest vulnerability to climate change: A review for future research framework. Forests 13 (6), 917. http://dx.doi.org/10.3390/f13060917.

Rouse, J.W., Haas, R.H., Schell, J.A., Deering, D.W., 1974. Monitoring Vegetation Systems in the Great Plains with ERTS. Nasa Special Publication, pp. 309–317.

Rousi, E., Kornhuber, K., Beobide-Arsuaga, G., Luo, F., Coumou, D., 2022. Accelerated western European heatwave trends linked to more-persistent double jets over Eurasia. Nat. Commun. 13 (1), 3851. http://dx.doi.org/10.1038/s41467-022-31432-y.

Russo, S., Sillmann, J., Fischer, E.M., 2015. Top ten European heatwaves since 1950 and their occurrence in the coming decades. Environ. Res. Lett. 10 (12), 124003. http://dx.doi.org/10.1088/1748-9326/10/12/124003.

Savitzky, A., Golay, M.J.E., 1964. Smoothing and differentiation of data by simplified least squares procedures. Anal. Chem. 36 (8), 1627–1639. http://dx.doi.org/10.1021/ac60214a047.

Schickhoff, U., Eschenbach, A., 2018. Terrestrische und semiterrestrische Ökosysteme. In: von Storch, H., Meinke, I., Claußen, M. (Eds.), Hamburger Klimabericht - Wissen Über Klima, Klimawandel Und Auswirkungen in Hamburg Und Norddeutschland. In: Springer eBook Collection, Springer, Berlin and Heidelberg, pp. 109–145. http://dx.doi.org/10.1007/978-3-662-55379-4_6.

Schütt, A., Becker, J.N., Reisdorff, C., Eschenbach, A., 2022. Growth response of nine tree species to water supply in planting soils representative for urban street tree sites. Forests 13 (6), 936. http://dx.doi.org/10.3390/f13060936.

Shahtahmassebi, A.R., Li, C., Fan, Y., Wu, Y., lin, Y., Gan, M., Wang, K., Malik, A., Blackburn, G.A., 2021. Remote sensing of urban green spaces: A review. Urban For. & Urban Green. 57, 126946. http://dx.doi.org/10.1016/j.ufug.2020.126946.

Shyrokaya, A., Messori, G., Pechlivanidis, I., Pappenberger, F., Cloke, H.L., Di Baldassarre, G., 2024. Significant relationships between drought indicators and impacts for the 2018–2019 drought in Germany. Environ. Res. Lett. 19 (1), 014037. http://dx.doi.org/10.1088/1748-9326/ad10d9.

Statistisches Bundesamt, 2025a. Bevölkerung: Bundesländer, Stichtag. URL: https://www-genesis.destatis.de/datenbank/online/table/12411-0010/search/s/MTI0MTEtMDAxMA== (Accessed: 31 March 2025).

Statistisches Bundesamt, 2025b. Bevölkerung: Gebietsfläche: Kreise, Stichtag. URL: https://www-genesis.destatis.de/datenbank/online/statistic/11111/table/11111-0002/search/s/MTExMTE= (Accessed: 31 March 2025).

Stirling, E., Fitzpatrick, R.W., Mosley, L.M., 2020. Drought effects on wet soils in inland wetlands and peatlands. Earth-Sci. Rev. 210, 103387. http://dx.doi.org/10.1016/j.earscirev.2020.103387.

Süßel, F., Brüggemann, W., 2021. Tree water relations of mature oaks in southwest Germany under extreme drought stress in summer 2018. Plant Stress. 1, 100010. http://dx.doi.org/10.1016/j.stress.2021.100010.

Teuling, A.J., Seneviratne, S.I., Stöckli, R., Reichstein, M., Moors, E., Ciais, P., Luyssaert, S., van den Hurk, B., Ammann, C., Bernhofer, C., Dellwik, E., Gianelle, D., Gielen, B., Grünwald, T., Klumpp, K., Montagnani, L., Moureaux, C., Sottocornola, M., Wohlfahrt, G., 2010. Contrasting response of European forest and grassland energy exchange to heatwaves. Nat. Geosci. 3 (10), 722–727. http://dx.doi.org/10.1038/ngeo950.

Thomsen, S., Reisdorff, C., Gröngröft, A., Jensen, K., Eschenbach, A., 2020. "Responsiveness of mature oak trees (Quercus robur L.) to soil water dynamics and meteorological constraints in urban environments". Urban Ecosyst. 23 (1), 173–186. http://dx.doi.org/10.1007/s11252-019-00908-z.

Trugman, A.T., Anderegg, L.D.L., Anderegg, W.R.L., Das, A.J., Stephenson, N.L., 2021. Why is Tree Drought Mortality so Hard to Predict? Trends Ecol. Evol. 36 (6), 520–532. http://dx.doi.org/10.1016/j.tree.2021.02.001.

Trugman, A.T., Detto, M., Bartlett, M.K., Medvigy, D., Anderegg, W.R.L., Schwalm, C., Schaffer, B., Pacala, S.W., 2018. Tree carbon allocation explains forest drought-kill and recovery patterns. Ecol. Lett. 21 (10), 1552–1560. http://dx.doi.org/10.1111/ele.13136.

Van Boxtel, et al., 2021. Gsignal: Signal processing. URL: https://github.com/gjmvanboxtel/gsignal.

Varghese, D., Radulović, M., Stojković, S., Crnojević, V., 2021. Reviewing the Potential of Sentinel-2 in Assessing the Drought. Remote. Sens. 13 (17), 3355. http://dx.doi.org/10.3390/rs13173355.

Vicedo-Cabrera, A.M., Scovronick, N., Sera, F., Royé, D., Schneider, R., Tobias, A., Astrom, C., Guo, Y., Honda, Y., Hondula, D.M., Abrutzky, R., Tong, S., de Sousa Zanotti Stagliorio Coelho, M., Saldiva, P.H.N., Lavigne, E., Correa, P.M., Ortega, N.V., Kan, H., Osorio, S., Kyselý, J., Urban, A., Orru, H., Indermitte, E., Jaakkola, J.J.K., Ryti, N., Pascal, M., Schneider, A., Katsouyanni, K., Samoli, E., Mayvaneh, F., Entezari, A., Goodman, P., Zeka, A., Michelozzi, P., de'Donato, F., Hashizume, M., Alahmad, B., Diaz, M.H., de La Cruz Valencia, C., Overcenco, A., Houthuijs, D., Ameling, C., Rao, S., Di Ruscio, F., Carrasco-Escobar, G., Seposo, X., Silva, S., Madureira, J., Holobaca, I.H., Fratianni, S., Acquaotta, F., Kim, H., Lee, W., Iniguez, C., Forsberg, B., Ragettli, M.S., Guo, Y.L.L., Chen, B.Y., Li, S., Armstrong, B., Aleman, A., Zanobetti, A., Schwartz, J., Dang, T.N., Dung, D.V., Gillett, N., Haines, A., Mengel, M., Huber, V., Gasparrini, A., 2021. The burden of heat-related mortality attributable to recent human-induced climate change. Nat. Clim. Chang. 11 (6), 492–500. http://dx.doi.org/10.1038/s41558-021-01058-x.

Vicente-Serrano, S.M., Azorin-Molina, C., Peña-Gallardo, M., Tomas-Burguera, M., Domínguez-Castro, F., Martín-Hernández, N., Beguería, S., El Kenawy, A., Noguera, I., García, M., 2019. A high-resolution spatial assessment of the impacts of drought variability on vegetation activity in Spain from 1981 to 2015. Nat. Hazards Earth Syst. Sci. 19 (6), 1189–1213. http://dx.doi.org/10.5194/nhess-19-1189-2019.

Vicente-Serrano, S.M., Beguería, S., López-Moreno, J.I., 2010. A multiscalar drought index sensitive to global warming: The standardized precipitation evapotranspiration index. J. Clim. 23 (7), 1696–1718. http://dx.doi.org/10.1175/2009JCLI2909.1.

Vicente-Serrano, S.M., Beguería, S., Lorenzo-Lacruz, J., Camarero, J.J., López-Moreno, J.I., Azorin-Molina, C., Revuelto, J., Morán-Tejeda, E., Sanchez-Lorenzo, A., 2012. Performance of drought indices for ecological, agricultural, and hydrological applications. Earth Interactions 16 (10), 1–27. http://dx.doi.org/10.1175/2012EI000434.1.

Vicente-Serrano, S.M., Camarero, J.J., Azorin-Molina, C., 2014. Diverse responses of forest growth to drought time–scales in the n orthern h emisphere. Glob. Ecol. Biogeogr. 23 (9), 1019–1030. http://dx.doi.org/10.1111/geb.12183.

Vicente-Serrano, S.M., Gouveia, C., Camarero, J.J., Beguería, S., Trigo, R., López-Moreno, J.I., Azorín-Molina, C., Pasho, E., Lorenzo-Lacruz, J., Revuelto, J., Morán-Tejeda, E., Sanchez-Lorenzo, A., 2013. Response of vegetation to drought time-scales across global land biomes. Proc. Natl. Acad. Sci. USA 110 (1), 52–57. http://dx.doi.org/10.1073/pnas.1207068110.

Vogelbacher, A., Aminzadeh, M., Madani, K., Shokri, N., 2024. An analytical framework to investigate groundwater–atmosphere interactions influenced by soil properties. Water Resour. Res. 60 (4), http://dx.doi.org/10.1029/2023WR036643.

West, H., Quinn, N., Horswell, M., 2019. Remote sensing for drought monitoring & impact assessment: Progress, past challenges and future opportunities. Remote Sens. Environ. 232, 111291. http://dx.doi.org/10.1016/j.rse.2019.111291.

West, H., Quinn, N., Horswell, M., White, P., 2018. Assessing vegetation response to soil moisture fluctuation under extreme drought using sentinel-2. Water 10 (7), 838. http://dx.doi.org/10.3390/w10070838.

Wilcoxon, F., 1945. Individual Comparisons by Ranking Methods. Biom. Bull. 1 (6), 80. http://dx.doi.org/10.2307/3001968.

Wilhite, D.A., Glantz, M.H., 1985. Understanding: the Drought Phenomenon: The Role of Definitions. Water Int. 10 (3), 111–120. http://dx.doi.org/10.1080/02508068508686328.

Wolf, S., Keenan, T.F., Fisher, J.B., Baldocchi, D.D., Desai, A.R., Richardson, A.D., Scott, R.L., Law, B.E., Litvak, M.E., Brunsell, N.A., Peters, W., van der Laan-Luijkx, I.T., 2016. Warm spring reduced carbon cycle impact of the 2012 US summer drought. Proc. Natl. Acad. Sci. USA 113 (21), 5880–5885. http://dx.doi.org/10.1073/pnas.1519620113.

Wu, C., Zhong, L., Yeh, P.J.-F., Gong, Z., Lv, W., Chen, B., Zhou, J., Li, J., Wang, S., 2024. An evaluation framework for quantifying vegetation loss and recovery in response to meteorological drought based on SPEI and NDVI. Sci. Total. Environ. 906, 167632. http://dx.doi.org/10.1016/j.scitotenv.2023.167632.

Zandler, H., Samimi, C., 2024. Cooling potential of urban tree species during extreme heat and drought: A thermal remote sensing assessment. Remote. Sens. 16 (12), 2059. http://dx.doi.org/10.3390/rs16122059.

Zhang, Z., Paschalis, A., Mijic, A., 2021. Planning London's green spaces in an integrated water management approach to enhance future resilience in urban stormwater control. J. Hydrol. 597, 126126. http://dx.doi.org/10.1016/j.jhydrol.2021.126126.

Zhu, L., Suomalainen, J., Liu, J., Hyyppä, J., Kaartinen, H., Haggren, H., 2017. A review: Remote sensing sensors: 2. In: Rustamov, R.B., Hasanova, S., Zeynalova, M.H. (Eds.), Multi-Purposeful Application of Geospatial Data. IntechOpen, London, http://dx.doi.org/10.5772/intechopen.71049.

Zhu, Z., Woodcock, C.E., 2012. Object-based cloud and cloud shadow detection in Landsat imagery. Remote Sens. Environ. 118, 83–94. http://dx.doi.org/10.1016/j.rse.2011.10.028.

Zhu, Z., Woodcock, C.E., 2014. Continuous change detection and classification of land cover using all available landsat data. Remote Sens. Environ. 144, 152–171. http://dx.doi.org/10.1016/j.rse.2014.01.011.

Zscheischler, J., Fischer, E.M., 2020. The record-breaking compound hot and dry 2018 growing season in Germany. Weather. Clim. Extrem. 29, 100270. http://dx.doi.org/10.1016/j.wace.2020.100270.

Zscheischler, J., Seneviratne, S.I., 2017. Dependence of drivers affects risks associated with compound events. Sci. Adv. 3 (6), e1700263. http://dx.doi.org/10.1126/sciadv.1700263.

Zscheischler, J., Westra, S., van den Hurk, B.J.J.M., Seneviratne, S.I., Ward, P.J., Pitman, A., AghaKouchak, A., Bresch, D.N., Leonard, M., Wahl, T., Zhang, X., 2018. Future climate risk from compound events. Nat. Clim. Chang. 8 (6), 469–477. http://dx.doi.org/10.1038/s41558-018-0156-3.